Far-Infrared Cyclotron Resonance of n-Type InSb under Electric Field

- Banding of Impurity State in Magnetic Field -

Yasuo Oka

March 1970

ABSTRACT

The shallow level impurity in n-type InSb in magnetic field has been investigated by means of far-infrared cyclotron resonance under electric field at low temperature. Variation of the resistivity with electric field under various magnetic field has also been measured and compared with the data on the cyclotron resonant experiments. In the case of high impurity concentration, the separation of the impurity state from the conduction band is only observable above a certain high magnetic field. However in the low concentration case, the impurity state is clearly separated from the conduction band even at low magnetic field. These experimental results demonstrate the necessity to take the effect of banding of the impurity state into consideration and support two-band model of n-type InSb suggested recently by several investigators from their transport experiments. The screening effect by conduction electrons in n-type InSb has been also studied. However, the present experimental results could not determine the strength of the effect. Magnetic field dependence of the impurity band has been investigated from the structure in the optical spectra. The banding and separation of the impurity state with magnetic field were confirmed. The experimental results are analysed by using the theory of the isolated state of impurity in strong magnetic field and also compared with the theory of impurity banding in magnetic field.

CONTENTS

§. 1 Introduction

The electrical conduction in semiconductors at low temperatures has been studied by many investigators for the purpose of making clear the mechanism of the impurity conduction. In the last ten years, various informations on this problem have been accumulated. However still now opposite proposals have been advocated on the basic point of this problem and the complete consistent understandings about the problem have not been established. The results hitherto obtained by many investigators indicate that the phenomena of the impurity conduction can be classified into three types of the conduction depending on the concentration of impurity; hopping region, intermediate region, and metallic region. The problem discussed recently is the relation between the impurity band produced from the impurity centers and the main band of the host lattice in the intermediate and the metallic regions. There have been such questions whether the density of state of the impurity band continues to the main band or not in these regions of impurity concentration and whether only the main band should be taken into consideration for the metallic conduction or both main band and impurity band should be.

In the systematic study of the problem there is one difficulty from the experimental point of view, that is, to control the concentration of impurity in the specimens for our purpose. Even with the present highly developed technique in the preparation of the crystals, it is not easy to eliminate the effect of unnecessary impurities and the effect of the compensation between donors and undoped acceptors (or vice versa), which disturbs studies on the concentration dependence of the impurity conduction. Therefore if the control of the concentration of impurity be possible following our purpose, the investigation of impurity conduction may be done more systematically and more satisfactorily.

Among the semiconductor materials, InSb is a representative III-V compound semiconductor. This substance has been a subject of precise study in semiconductor physics. The remarkable characteristics of this material are; the small effective mass of conduction band electron ($m^* \sim 0.014\ m_o$) originated in the nallow band gap which produces strong repulsive force between the conduction band and the valence band and the large value of the g-factor of the conduction band electron ($g \sim -50$) resulted in the strong spin-orbit coupling. The smallness of the ionization energy of the hydrogenic donor impurity in InSb ($E_i \sim 0.7$ meV) is attributed to the small effective mass of electron. In the study of the effect of external magnetic field upon the electron bound to this donor, the ratio,

$$\gamma = \hbar\omega_c / 2E_i \ ,$$

will be used as a good measure of the efficiency of the magnetic field, where $(1/2)\hbar\omega_c$ is the zero point energy of electron in magnetic field (ω_c is the angular frequency of cyclotron motion). The strength of the magnetic field which satisfy the condition $\gamma = 1$ is about 1900 Oe for the donor electron in InSb whereas for the donors in Ge the strength is about 40 times larger and for the hydrogen atom, 10^6 times larger than that of the donor electron in InSb.

This estimation indicates that the condition of the sufficient strong magnetic field, $\gamma > 1$, can be easily realized for the donor state in InSb by using conventional magnetic field. In the condition of $\gamma > 1$, the wave function of electron bound to the donor atom may be modulated by external field; the orbit of the donor electron perpendicular to the magnetic field is shrinked as the magnetic field is increased. Therefore the overlapping of the wave function of the donor electron to

that in the nearest neighbour impurities can be reduced by external magnetic field and this condition may considered to correspond effectively to the reduction of donor concentration.

N-type InSb is very convenient to study the problem of the impurity conduction, since the overlapping of wave functions, therefore the effective donor concentration, can be changed by the external magnetic field. According to the consideration described above, the impurity state and the impurity conduction of n-type InSb in magnetic field have been investigated and will be discussed.

The formation of the impurity band in n-type InSb in magnetic field was reported for the first time by Sladek,[1] who studied this problem by means of transport phenomena. Thereafter, many experiments on this material was made from the various point of view. The general conception concluded from these results is that even in the purest specimen usually avairable, not less than 1×10^{14} cm^{-3} of donor concentration, donor states are merged into the conduction band in the case of zero magnetic field. Namely, this material has been considered to be a typical degenerate semiconductor. Only in the case of strong magnetic field applied it was considered that the electronic state of donor is modified obviously and the electrons are bound to the donor state at an amount of magnetic field. The process is called as "freezeout effect".

Contrary to these concepts, Lien Chih-ch'ao and Nasledov[2] and Miyazawa and Ikoma[3] presented another proposal from the transport experiment. They demonstrated that in the case of donor concentration of 1×10^{14} cm^{-3} the impurity band is formed and split from the conduction band even at zero magnetic field. Especially Miyazawa and Ikoma have analyzed the temperature and magnetic field dependence of the Hall coefficient and resistivity by introdusing two-band model and showed detailed informations on the properties of the impurity band.

On the other hand, Boyle and Brailsfold[4] studied the optical absorption of n-type InSb in magnetic field and attributed the satellite absorption line which appears near the cyclotron resonant frequency of free electron to the transition between the impurity states associated with the Landau levels of the free electron. Recently Kaplan[5] et al. and Dickey et al.[6] have investigated the resonant absorptions near the cyclotron frequencies and the absorptions near the ionization energy of donors and reported various interesting results on the impurity state in strong magnetic field. The results obtained from the optical experiments were well interpreted as phenomena of the isolated state of impurity. The magnetic field used in their optical experiments was considerebly stronger than that used in the transport experiments mentioned before. Therefore the impurity state in magnetic field can be considered to alter its character from band to isolated level with increase of applied magnetic field.

In strong magnetic field at low temperature resistivity of n-type InSb exhibits a sharp drop at a certain electric field. As for the origin of this non-linearity of the resistance, different interpretations have been advocated. One is presented by several investigators[7,8,9] who support the degenerate model of impurity state and the other is by investigators[1,2,3,10] who believe the existance of the separated impurity band: The former interprete the resistivity drop as a change of the scattering mechanism in hot electrons. Recently Yamada and Kurosawa[11] have published a theory on the non-linearity based on the degenerate model. The latter attributed the phenomenon to the impact ionization of electrons from the freezeout state of impurity.

In the present paper the author wish to make the origin of the non-linearity of the resistance clear and to study banding processes of

of the impurity state in magnetic field by means of electric field dependence of cyclotron resonant absorptions. The results will be discussed in comparison with the theories of the isolated state of impurity and with the recent theory of impurity band in magnetic field.

§. 2 Experimental Procedures

Far-infrared cyclotron resonant absorption of n-type InSb under electric field was studied at liquid helium temperature. Measurements of electric field dependence of the resistivity were also made in the same condition and relationships between both results was examined. The far-infrared spectrometer employed was Hitach model FIS-21. The monochromatic light was introduced to the specimen by using light pipe systems. A schematic diagram of the system in the present experiment is shown in Fig. 1. The diameter of the light pipes was 10 mm. A superconducting magnet of Nb-Zr was used for the measurement in magnetic field. For the transmission measurement, Ge detectors of either photoconductivity type or bolometer type were available.[12] Signals from detector were amplified by a lock-in amplifier and recorded. The temperature dependence of the optical absorption and resistivity was studied by changing the vapour pressure of the liquid helium or by Joule heating of a heater wire situated under the specimen. Electric field was applied through the electrodes to the specimen.

Samples used in this experiment were cut from single crystal ingots of n-type InSb and the effective donor concentration, $N_D - N_A$, was in the range of $7.5 \times 10^{12} \sim 1.7 \times 10^{15}$ cm^{-3}. As shown in Table 1, two purer samples were undoped and the dopant of the other one was Te impurity. The samples cut from ingots were lapped with carborundum and etched with CP-4A and then indium metal was soldered at the edges of the sample as electrode. Ohmic properties of electrode-sample contact was tested by alternating applied current direction. The dimension of each sample was about 5 mm in width and about 6 mm in length and $150 \sim 200$ microns in thickness. To aboid temperature

rise in the sample due to Joule heating in the case of applying electric field, helium gas was filled in the light pipe system as a exchange gas. However Ge-bolometer was only available[12] in a evacuated condition of the system.

In the present experiments of cyclotron resonant absorption, the wavelength of far-infrared light was varied near the cyclotron resonant frequencies under constant magnetic field which was directed in Faraday configuration. For the purpose of the observation of electric field dependence of the resonant absorption, static electric field transverse to the magnetic field was applied through the electrodes of the sample. The sample,TE 7512, was used only for measurements of cyclotron resonance by means of photoconductivity response and the results were compared with the other transmission data. Though the effective donor concentration of TE 7512 was smallest among those used in our experiment ($N_D - N_A = 7.5 \times 10^{12}$ cm^{-3}), the real donor impurity consentration, N_D, was considered to be more than 10^{14} cm^{-3} due to its high compensation.

§. 3 Experimental Results

3 - 1. Preliminaries

The resonant frequencies observed in the present experiment are schematically shown by the arrows in Fig. 2. The Landau levels of free electron of Landau quantum number, n = 0, with up-spin and down-spin are symbolized by (0, ↑) and (0, ↓) respectively, and the levels of n = 1 with up-spin and down-spin are represented by (1, ↑) and (1, ↓) respectively. Under the bottom of each Landau level of free electron, there exist impurity states associated with the Landau levels and they are confirmed by cyclotron resonant measurements. The impurity states associated with (0, ↑) and (1, ↑) are designated as (000) and (110) respectively. For the spin down state, similar impurity states may be associated with. However, these states have not important role in the present experiment, therefore they are neglected. The assignment of the impurity states was given by Wallis and Bowlden[13] and Hasegawa and Howard[14] for the isolated states of impurity.*) The transition from (000) to (110) is named ω_I and that from (0, ↑) to (1, ↑), $\omega_{c\uparrow}$. $\omega_{c\downarrow}$ is also given for the similar transition between down-spin states. According to Hasegawa-Howard, the oscillator strength from (000) to (110) is unity in the condition of strong magnetic field. Therefore

---

*) In this paper, the author uses the notation of the quantum number (n,m,λ) used by Hasegawa and Howard, instead of (ℓ,m,λ) used by Wallis and Bowlden. The relation between n and ℓ is given by

$$n = \ell + \frac{1}{2}(|m| + m).$$

the main transition from (000) is restricted to that to (110) in the present experiment.

3 - 2. Electric Field Dependence of Resistivity in Transverse Magnetic Field

Miyazawa and Ikoma have reported that, in the case of the donor-concentration of 10^{14} cm^{-3}, current-voltage curve on InSb exhibits non-linearity and temperature dependence even in zero magnetic field. This characteristics are emphasized by increasing the transverse magnetic field intensity. The electric field dependences of the resistivity of MO 1814 and TE 1715 in several magnetic field strengths are shown in Fig. 3 and Fig. 4. The temperatures of the samples were 1.8 ^{o}K and 4.2 ^{o}K, and the magnetic field applied was less than 30 KOe. The main discrepancy of resistivity vs. electric field characteristics between these two samples of different impurity-concentration appears at relative low magnetic field. For the sample of high impurity concentration, TE 1715 (Fig. 4), the resistivity is thoroughly constant in wide ranges of both electric field and temperature when the magnetic field is not exceeded to 10 KOe. However, this is not true at high magnetic field, i.e., at 19.3 KOe and 27.6 KOe. At high magnetic field a sudden drop of the resistivity takes place at about 1 V/cm of electric field and the magnitude of this resistivity-drop becomes larger as temperature is lowered down to 1.8 ^{o}K.[10] On the contrary, in the case of MO 1814 (Fig. 3), even at zero magnetic field there appear non-linearity and temperature dependence of current-voltage curve which are observed only at strong magnetic field in the samples of high impurity

concentration. As already mentioned, we have had two kinds of interpretations about the non-ohmic property in n-type InSb in strong magnetic field at low temperature; one of them is based on a hot electron effect in degenerate semiconductors,[7,8,9] and the other is based on impact ionization of electrons from the freeze-out states of impurity.[1,2,3] For the purpose to study the origin of the non-linearity, we carried out the following experiment.

3 - 3. Electric Field Dependence of Resonant Absorptions

Transmission measurements of n-type InSb in far-infrared region under electric field were done on the two kinds of samples mentioned in the preceding section. The ratios of the transmission in magnetic field to that at zero field, $T(H)/T(0)$, are plotted against the wave number as shown in Figs. 5, 6, 7, and 8.

i) Low-Impurity-Concentration Case, MO 1814

The resonant absorption spectra of MO 1814 at 1.8 ^{o}K and 4.6 KOe are shown in Fig. 5. In a thermal equilibrium without electric field, the transmission spectra showed a characteristic indicated by a solid curve in the figure and the peak wave number corresponds to the transition between the impurity states associated with the Landau levels of free electron, ω_I. On the way to increasing applied electric field, the transmission spectrum showed a remarkable change at the field region of the resistivity drop. The absorption maximum in the dashed curve corresponds to the spin-up cyclotron resonant frequency of free electron, $\omega_{c\uparrow}$. This result demonstrates that in the case of strong electric

field almost all of the electron in the impurity states are removed to conduction band and it is natural to consider that the removement originates in an impact ionization. In the range of magnetic field strength above mentioned, the impurity states can be considered to separate clearly from the conduction band since the observed resonant transitions corresponding to the two transitions, ω_I and $\omega_{c\uparrow}$, are really distinguishable.

In Fig. 6 resonant transmission spectra on the same sample at 4.2 ^{o}K and at 19.3 KOe are shown. Clear resolution between the transmission minima corresponding to ω_I and $\omega_{c\uparrow}$ can be seen at E = 0 V/cm as shown by the solid curve. As the temperature is lowered to 1.8 ^{o}K the absorption corresponding to $\omega_{c\uparrow}$ is known to disappear. On the other hand, if the electric field is increased to 3.9 V/cm which corresponds to the condition just over the resistivity-drop, the absorption related to $\omega_{c\uparrow}$ increases remarkably and that related to ω_I decreases considerably as shown by a dashed curve in the figure. At high electric field, 6.0 V/cm, the absorption corresponding to ω_I decreases appreciably, and the absorption corresponding to $\omega_{c\downarrow}$ is newly observed. These behaviours are shown by the dash-dotted curve in Fig. 5.

The changes in the transmission spectra with applied electric field are considered to be originated in the changes of electron population in the states, (000), (0, $\uparrow$), and (0, $\downarrow$). Both the increase of electron temperature by impact ionization and the increase of lattice temperature by Joule heating may cause the repopulation of the electron. We attempted to make measurement of spectral change in other experimental condition. When lattice temerature of the sample was raised by an external heater, the relative intensities of the absorptions corresponding

to ω_I and $\omega_{c\downarrow}$ with that corresponding to $\omega_{c\uparrow}$ vary in somewhat different manner from the case of applying electric field. In the case of external heating, namely the lattice temperature raising, the absorption corresponding to ω_I almost disappeared at the temperature where the absorption corresponding to $\omega_{c\downarrow}$ began to appear, i.e., we could not observe the absorptions corresponding to ω_I and $\omega_{c\downarrow}$ simultaneously. Therefore, in the present experiment on electric field effect, the electron distribution deviates appreciably from Maxwell-Boltzmann's law which is applicable only in thermal equilibrium cases. In high electric field electrons may become hot enough to populate to (0, $\downarrow$) Landau level by impact ionization.

For the sample of donor concentration of 10^{14} cm^{-3}, the impurity state is optically distinguishable from the Landau level of free electron even at relatively low magnetic field. This is consistent with the transport data shown in Fig. 3. However, by the present method of cyclotron resonance, we can not confirm the separation at zero magnetic field.

ii) High-Impurity Concentration Case, TE 1715

The transmission spectra of TE 1715, the effective donor concentration of which is 1.7×10^{15} cm^{-3}, at 1.8 ^{o}K and at 10.1 KOe are shown in Fig. 7. As we have known from Fig. 4, the resistivity of this sample does not show any change with the change of either electric field or temperature in the magnetic field of 10.1 KOe. In the resonant transmission spectrum in zero electric field, the curve has only one broad absorption maximim and we can not distinguish two peaks due to ω_I and $\omega_{c\uparrow}$ as shown by solid curve. Application of electric field causes little change on the spectral line shape and the wave

number of absorption maximum as shown by the dashed curve in Fig. 7. The transmission spectrum of MO 1814 in the same magnetic field is also presented as a comparison by a narrow dashed curve in the figure. For the sample of MO 1814 of smaller carrier-concentration, the separation between the two absorption peaks is known to be much clear. Moreover from the comparison, it can be found that the wave number of the maximum absorption for TE 1715 does not correspond with $\omega_{c\uparrow}$ but with ω_I. This result may be interpreted as follows: The impurity states in TE 1715 form a band and the energy states distribute continuously to the Landau levels of free electron. In such a case, two bands can not be distinguishable and the excitation of electron by impact may not be expected. Consequently, the center of the state-density of the impurity, therefore the center of the electron population, situates at the same energy point as in the localized condition of the impurity state. These experimental results are consistent with the measurement about the density of the impurity band by means of tunneling experiment of GaAs.[15)]

The transmission spectra of TE 1715 at 1.8 ^{o}K and at 19.3 KOe are shown in Fig. 8. For the sample in this condition, the resistivity drop has been known to be observed as shown in Fig. 4. Two absorption peaks can be distinguished and over the electric field of the resistivity-drop, at E = 1.17 V/cm, the intensities of the absorption at the two peaks interchanges. From the result, it is known that in the magnetic field intensity, a dip of the density of state is produced between the impurity state and the Landau level of free electron. In the same figure, resolved spectra from the solid curve to those related to ω_I and $\omega_{c\uparrow}$ are shown by a narrow dashed curve.

The magnetic field dependence of the energy related to ω_I and $\omega_{c\uparrow}$ are shown in Fig. 9. As is well known, the curve of the cyclotron resonance of free electron bends downward with increasing of the magnetic field strength, because of the non-parabolicity of the conduction band.[16] The energy related to ω_I are known to be a little higher than those to $\omega_{c\uparrow}$. The effective mass derived from the linear part of the curve related to $\omega_{c\uparrow}$ is 0.0143 m_o.

Recently Yamamoto[17] studied the similar electric field dependence of the optical absorption by the photoconductivity responce. The present experimental results are consistent with his results. The spectral line-width by Yamanoto is much broader than that of the present results. This discrepancy may be explained by the difference of the compensation ratio of the specimens.

§. 4 Comparison with Theory and Discussion

4 - 1. Preliminaries

On the hydrogenic impurity state in strong magnetic field, we have a well known theory by Yafet, Keyes, and Adams (Y.K.A.).[18] Wallis and Bowlden (W-B)[13] reported the calculation with the same kind of variational methods and extended the calculation to the various excited levels and to the upper Landau levels. They simplified the theory of Y.K.A. by using only one variational parameter and the another variational parameter which corresponds to the spread of the wave function perpendicular to the magnetic field was replaced with the cyclotron orbit of free electron. Hasegawa and Howard (H-H)[14] solved the problem in the accurate form at the infinite limit of the magnetic field. One of the important conclusion by H-H is that the transition from (000) is restricted to that to (110) for left circularly polarized light (l.c.p.) in the condition of strong magnetic field. In the cyclotron resonance of free electron, the oscillator strength of the transition, $\Delta n = 1$, is unity for l.c.p. ignoring the non-parabolicity of the conduction band. Therefore in the present experimental condition it is reasonable to assume that the oscillator strengths for ω_I and $\omega_{c\uparrow}$ are nearly unity.

In the section 4 - 2, the present experimental results will be compared with the theory based on the model of isolated impurity. Some advancement from the usual theory will be made. In the section 4 - 3 the author will formulate the effect of the screening by conduction electrons on the impurity state and the results will be compared with the experiment. The comparison with the recent theory of impurity

band in magnetic field will be made in the section 4 - 4.

4 - 2. Isolated Impurity State in Strong Magnetic Field

The electronic state of the shallow level impurity in magnetic field can be descrived by the following manner: The Hamiltonian of one electron which sees the Coulomb potential of the monovalent impurity atom in the lattice (static dielectric constant : κ) in magnetic field is given by

$$\mathcal{H}_o = \frac{1}{2m^*}\left(P + \frac{e}{c} A \right)^2 - \frac{e^2}{\kappa R}, \qquad (4.2.1)$$

where m^* is a effective mass of electron and A is the vector potential. When we choose the gauge that $A = (-yH/2, xH/2, 0)$, (4.2.1) is rewritten as follows:

$$\mathcal{H}_o = \frac{p^2}{2m^*} + \frac{eH}{2m^*c}(xP_y - yP_x) + \frac{m^*}{8}\left(\frac{eH}{m^*c}\right)^2 (x^2 + y^2) - \frac{e^2}{\kappa R}. \qquad (4.2.2)$$

By using the effective Rydberg ($Ry^* = m^* e^4 / 2\hbar^2\kappa^2$) and the effective Bohr radius ($a_B^* = \kappa\hbar^2 / m^* e^2$) as units of energy and length respectively, the Hamiltonian (4.2.2) is normarized in dimension less form and is expressed in cylindrical coordinates (ρ, ϕ, z)

$$\mathcal{H} = -\nabla^2 - i\gamma \frac{\partial}{\partial \phi} + \gamma^2 \frac{\rho^2}{4} - \frac{2}{r} , \qquad (4.2.3)$$

where $\gamma = \hbar \omega_c / 2Ry^*$, $\omega_c = eH / m^*c$, $p = -i\hbar\nabla$, and $r^2 = \rho^2 + z^2$. By using variational method, Y.K.A. calculated magnetic field dependence of the energy of the (000) state which is the ground state of impurity associated with the lowest Landau level. They adopted the following trial function of the correct symmetry for (000):

$$\Psi_{000}(\rho, \phi, z) = \left(\frac{1}{2^{3/2} a_\perp^2 a_\parallel \pi^{3/2}} \right)^{1/2} \exp\left(- \frac{\rho^2}{4a_\perp^2} \right) \times \exp\left(- \frac{z^2}{4a_\parallel^2} \right) , \qquad (4.2.4)$$

where $a_\parallel$ and $a_\perp$ are the variational parameters parallel and perpendicular to the magnetic field. Trial value of the energy of the (000) state is given by

$$\langle E_{000} \rangle = \frac{1}{2a_\perp^2} \left(1 + \frac{\varepsilon^2}{2} \right) + \frac{\gamma^2 a_\perp^2}{2} - \sqrt{\frac{2}{\pi}} \frac{\varepsilon}{a_\perp (1 - \varepsilon^2)^{1/2}} L_n(\varepsilon) , \qquad (4.2.5)$$

where

$$\varepsilon = a_\perp / a_\parallel ,$$

and

$$L_n(\varepsilon) = \ln \frac{1 + (1 - \varepsilon^2)^{1/2}}{1 - (1 - \varepsilon^2)^{1/2}} .$$

From the condition to minimize the trial value of $\langle E_{000} \rangle$ with respect to $a_\perp$ and ε, i.e., $\partial \langle E_{000} \rangle / \partial a_\perp = 0$ and $\partial \langle E_{000} \rangle / \partial \varepsilon = 0$, following two relations are obtained:

$$a_\perp = \sqrt{\frac{\pi}{2}} \frac{\varepsilon}{2} (1 - \varepsilon^2)^{3/2} \frac{1}{L_n(\varepsilon) - 2(1 - \varepsilon^2)^{1/2}} , \qquad (4.2.6)$$

and

$$\gamma^2 = \frac{1}{a_\perp^4} (1 + \frac{\varepsilon^2}{2}) - \sqrt{\frac{2}{\pi}} \frac{\varepsilon}{a_\perp^3 (1 - \varepsilon^2)^{1/2}} L_n(\varepsilon). \qquad (4.2.7)$$

The binding energy, E_{000} is given by the differnce between the bottom of the lowest Landau level, (n = 0), and the expectation value of $\langle E_{000} \rangle$, namely

$$E_{000} = \gamma - \langle E_{000} \rangle . \qquad (4.2.8)$$

W-B extended the above theory of Y.K.A. to the excited levels and higher Landau levels. As is mentioned before, they replaced the one variational parameter, $a_\perp$, with the cyclotron orbit for simplifying the calculations. However it is known that this replacement is not necessarily good in the range of $\gamma < 10$ which is the condition of the present experiment. The calculation of the energy of (110) state using two variational parameters was reported briefly by Larsen.[19] However he did not show any explicit expression for the expectation value of the energy and the variational conditions. So we develop here this problem and show the analytic forms of the results on the state (110).

With regard to the wave function of the first excited state, (n = 1), of the harmonic oscillator the trial function of correct symmetry for the (110) state can be expressed as follows:

$$\Psi_{110}(\rho, \phi, z) = - \frac{1}{2\sqrt{\pi}\, a_\perp^2} \left(\frac{1}{2\pi\, a_{||}^2} \right)^{1/4} \exp(i\phi)$$

$$\times \rho \exp\left(- \frac{\rho^2}{4\, a_\perp^2} \right) \exp\left(- \frac{z^2}{4\, a_{||}^2} \right). \qquad (4.2.9)$$

Using this trial function, the trial value of the energy of (110) is given by

$$\langle E_{110} \rangle = \frac{1}{4\, a_\perp^2} (4 + \varepsilon^2) + \gamma + \gamma^2 a_\perp^2$$

$$- \frac{1}{\sqrt{2\pi}\, a_\perp} \varepsilon \left\{ \frac{2 - \varepsilon^2}{(1 - \varepsilon^2)^{3/2}} L_n(\varepsilon) - \frac{2}{1 - \varepsilon^2} \right\}. \qquad (4.2.10)$$

From the two variational conditions, following two relations are obtained:

$$a_\perp = \frac{\sqrt{2\pi}\, \varepsilon\, (1 - \varepsilon^2)^{5/2}}{2\,(2 + \varepsilon^2)} \frac{1}{L_n(\varepsilon) - \dfrac{6\,(1 - \varepsilon^2)^{1/2}}{2 + \varepsilon^2}}, \qquad (4.2.11)$$

and

$$\gamma^2 = \frac{1}{4\, a_\perp^4} (4 + \varepsilon^2) - \frac{\varepsilon}{2\sqrt{2\pi}\, a_\perp^3} \left\{ \frac{2 - \varepsilon^2}{(1 - \varepsilon^2)^{3/2}} L_n(\varepsilon) - \right.$$

$$- \frac{2}{1 - \varepsilon^2} \Bigg\} . \qquad (4.2.12)$$

The binding energy E_{110} is given by

$$E_{110} = 3\gamma - \langle E_{110} \rangle . \qquad (4.2.13)$$

For the purpose to compare these expressions with those of W-B, their formulae are shown. They replaced the parameter $a_\perp$ with $(1 / \gamma)^{1/2}$, (cyclotron orbit in Bohr unit) and used only one variational parameter, $\varepsilon = a_\perp / a_{||} = (1 / \gamma)^{1/2} / a_{||}$. For (000) state, trial function, trial value of the energy, and the relation obtained from the variational condition are given respectively by

$$\psi_{000}^{WB} = \frac{\gamma^{1/2}}{(2\pi)^{3/4} a_{||}^{1/2}} \exp\left(- \frac{\gamma}{4} \rho^2 \right) \exp\left(- \frac{z^2}{4 a_{||}^2} \right) , \qquad (4.2.14)$$

and

$$\langle E_{000} \rangle^{WB} = \gamma \left(1 + \frac{\varepsilon^2}{4} \right) - \sqrt{\frac{2\gamma}{\pi}} \frac{\varepsilon}{(1 - \varepsilon^2)^{1/2}} L_n(\varepsilon) , \qquad (4.2.15)$$

and

$$\sqrt{\frac{\pi \gamma}{2}} = \frac{2}{\varepsilon (1 - \varepsilon^2)^{3/2}} [L_n(\varepsilon) - 2 (1 - \varepsilon^2)^{1/2}] . \qquad (4.2.16)$$

(The expressions given by W-B are indicated by the sign of WB on the shoulders.)

Similarly for (110),

$$\Psi_{110}^{WB} = -\left(\frac{\gamma}{2\pi}\right)^{3/4} \varepsilon^{1/2} \left(\frac{\gamma}{2}\right)^{1/2} \exp(i\phi)$$

$$\times \rho \exp\left(-\frac{\gamma}{4}\rho^2\right) \exp\left(-\frac{z^2}{4a_{\parallel}^2}\right), \qquad (4.2.17)$$

and

$$\langle E_{110} \rangle^{WB} = \gamma\left(3 + \frac{\varepsilon^2}{4}\right) - \sqrt{\frac{\gamma}{2\pi}}\,\varepsilon\left\{\frac{2-\varepsilon^2}{(1-\varepsilon^2)^{3/2}} L_n(\varepsilon) - \frac{2}{1-\varepsilon^2}\right\}, \qquad (4.2.18)$$

and

$$\sqrt{\frac{\pi\gamma}{2}} = \frac{2+\varepsilon^2}{\varepsilon(1-\varepsilon^2)^{5/2}}\left[L_n(\varepsilon) - \frac{6(1-\varepsilon^2)^{1/2}}{2+\varepsilon^2}\right]. \qquad (4.2.19)$$

Replacing $a_{\perp}$ by $(1/\gamma)^{1/2}$, the formulae which use two parameters coinside with the above expressions.

Numerical values of the binding energies of (000) and (110), i.e., E_{000} and E_{110}, calculated by the above two methods are shown in Fig. 10. Comparing the result by two parameter method with that of W-B, the difference of both method for E_{110} is small. The reason of the small difference is explained by γ - dependence of the variational parameter as is shown in Fig. 11. In the one variational parameter method of W-B, the parameter $a_{\perp}$ is replaced by the cyclotron orbit $\ell_c = (1/\gamma)^{1/2}$. As far as the (110) state is

concerned, $a_\perp$ does not differ from ℓ_c even in the range of $\gamma \sim 1$. Contradictorily, for the (000) state, the difference between $a_\perp$ and ℓ_c is large near $\gamma \sim 1$ as is shown by Y.K.A.. In Fig. 12 γ - dependence of the variational parameters for (000) is shown (cf. Fig. 2 of Y.K.A.'s paper[18]).

The energy difference, $E_{000} - E_{110}$, in Fig. 10 should be equal to the energy difference between the two transition corresponding to ω_I and $\omega_{c\uparrow}$ in Fig. 9. This comparison is made in Fig. 13. In this figure the more advanced theoretical values of the energy difference calculated by Larsen[19] in the case of parabolic band is also shown. Here the theoretical values are fitted to experimental result by using the observed effective mass ($m^* = 0.0143\ m_o$), and the static dielectric constant, κ, is chosen to be 16. Therefore 1 Ry* = 0.76 meV. Recently Kaplan[20] reported the results for this energy difference. He measured the energy difference up to more higher magnetic field. He used the following values in his calculation, $m^* = 0.0138\ m_o$, $\kappa = 17$, and therefore, 1 Ry* = 0.6 meV. Consequently, his theoretical values are smaller than the values calculated by the author in Fig. 13. The variation of the static dielectric constant gives a delicate influence on the results of the calculation. He demonstrated the importance of the non-parabolicity of the conduction band and the central cell correction of the impurity potential from his other experimental results and made excellent works on the impurity state in strong magnetic field.

4 - 3. Screening Effect on the Isolated State of Impurity in Strong Magnetic Field.

In the preceding section, the experimental result of optical absorption was explained well by the theory of isolated state of impurity. However the binding energy of (000) derived from the transport experiment by Miyazawa and Ikoma was significantly smaller than that of Y.K.A.. The reason of this small binding energy was explained with the screening effect of the impurity potential by conduction electrons. Therefore, the influence of screening effect upon the result of the optical absorption should be examined.

Fenton and Haering[21] studied the effect of screening by conduction electrons on the isolated state of impurity in strong magnetic field. They carried out a variational calculation on the (000) state using Hamiltonisn in which the potential term was replaced with the screened Coulomb potential. In their calculation, if the trial function was the same form of Y.K.A. which is valid in strong field condition, the analytic form could not be derived for the expectation value of the energy. Therefore they treated this problem by using the wave function of 1 S - state of hydrogen atom in modified form, which is adequate in weak magnetic field limit.

As is shown in Fig. 13, for the binding energies, E_{000} and E_{110}, only the difference, $E_{000} - E_{110}$, is obtainable by the present experiment. In the study comparing the theory to the present experiment, the screening effect on the (110) state must be known as well as that on the (000) state. It is difficult to extend the method by Fenton and Haering to the (110) state which is the assosiated state with first excited Landau level, since they modified the wave function in zero magnetic field. Accordingly, in this paper, this problem is tried to solve by using the trial function

of W-B. The method of two parameters is not so significant comparing with the one parameter method in the case without screening (cf. Fig. 10).

The Hamiltonian of the problem is the similar form to (4.2.1) and only the potential term is replaced by the screened Coulomb potential, $-\left(e^2 / \kappa R \right) \exp\left(- R / \Lambda \right)$, where Λ is the screening length. By using the cylindrical coordinate, the dimensionless Hamiltonian, $\mathcal{H}_s$, is given by (cf. 4.2.3)

$$\mathcal{H}_s = - \nabla^2 - i \gamma \frac{\partial}{\partial \phi} + \gamma^2 \frac{\rho^2}{4} - \frac{2}{r} \exp\left(- \frac{r}{\lambda} \right), \qquad (4.3.1)$$

where $\lambda = \Lambda / a_B^*$.

The trial functions for (000) and (110) by W-B are given by (4.2.14) and (4.2.17) respectively. Using these functions the trial values are calculated for (4.3.1). Since the foregoing three terms of (4.3.1) are the same forms as those of (4.2.3), refering (4.2.15), the trial value of the energy of (000), $\langle E_{000} \rangle^s$, is

$$\langle E_{000} \rangle^s = \gamma \left(1 + \frac{1}{4} \varepsilon^2 \right) - \sqrt{\frac{1}{2\pi}} \gamma^{3/2} \varepsilon \int_0^\infty d\rho \int_{-\infty}^\infty dz$$

$$\times \rho \frac{2}{r} \exp\left(- \frac{r}{\lambda} \right) \exp\left(- \frac{\gamma}{2} \rho^2 \right) \exp\left(- \frac{1}{2} \gamma \varepsilon^2 z^2 \right) . \qquad (4.3.2)$$

(The sign , s, on the shoulder indicates the screening.)

To carry out the integration of the second term of the right hand

side of (4.3.2), let us now introduce the transformation of the variables.

$$\rho = \left(\frac{1}{\gamma} \right)^{1/2} a \cos \theta$$

$$z = \left(\frac{1}{\gamma \varepsilon^2} \right)^{1/2} a \sin \theta \quad . \qquad (4.3.3)$$

The Jacobian and the radial distance, r, become

$$\frac{\partial (\rho, z)}{\partial (a, \theta)} = \frac{a}{\gamma \varepsilon} \quad ,$$

and

$$r = \sqrt{\rho^2 + z^2} = \frac{a}{\gamma^{1/2} \varepsilon} \sqrt{\varepsilon^2 \cos^2 \theta + \sin^2 \theta} \quad . \qquad (4.3.4)$$

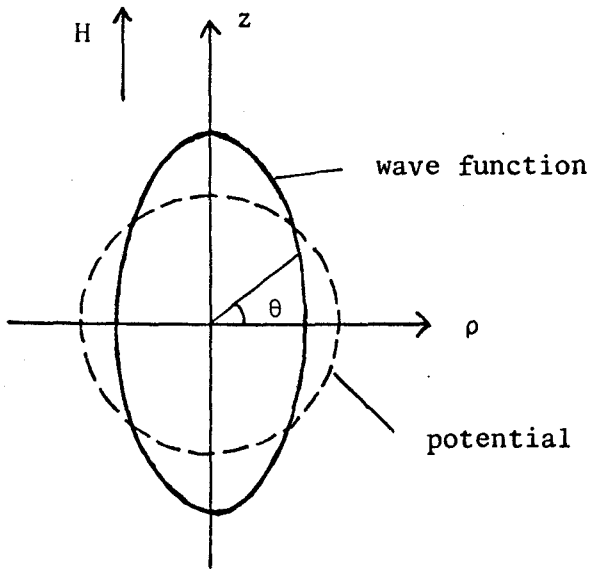

The second term (S.T.) of (4.3.2) is expressed by these new variables, a and θ , as follows:

$$(\text{S.T.}) = -\sqrt{\frac{1}{2\pi}}\; 2\,\gamma^{1/2}\varepsilon \int_0^{\infty} da \int_{-\pi/2}^{\pi/2} d\theta \; \frac{a \cos\theta}{\sqrt{\varepsilon^2 \cos^2\theta + \sin^2\theta}}$$

$$\times \exp\left(-\frac{1}{2} a^2 - \beta(\theta)\, a \right) \quad , \qquad (4.3.5)$$

where

$$\beta(\theta) = \frac{1}{\gamma^{1/2}\,\varepsilon\,\lambda} \sqrt{\varepsilon^2 \cos^2\theta + \sin^2\theta} \quad .$$

$\beta(\theta)$ shows the anguler, θ, dependence of the efficiency of the screening to the ellipsoidal wave function.

Since the double intergral in (4.3.5) can't be carried out simply, the following approximation is made on $\beta(\theta)$: First the term $(1 - \varepsilon^2)\cos^2\theta$ in square root is expanded.

$$\beta(\theta) = \frac{1}{\gamma^{1/2}\,\varepsilon\,\lambda} \sqrt{1 - (1 - \varepsilon^2)\cos^2\theta}$$

$$= \frac{1}{\gamma^{1/2}\,\varepsilon\,\lambda} \left\{ 1 - \frac{1}{2}(1 - \varepsilon^2)\cos^2\theta + \right.$$

$$\left. + \frac{1}{8}(1 - \varepsilon^2)^2 \cos^4\theta - \frac{1}{16}(1 - \varepsilon^2)^3 \cos^6\theta + \cdots \right\} . \qquad (4.3.6)$$

Then the averaged value β with regard to θ, is substituted in (4.3.5) instead of $\beta(\theta)$. From (4.3.6),

$$\beta \equiv \frac{2}{\pi} \int_0^{\pi/2} \beta(\theta)\, d\theta$$

$$= \frac{1}{\gamma^{1/2}\, \varepsilon\, \lambda} \left\{ 1 - \frac{1}{4}(1 - \varepsilon^2) + \frac{3}{64}(1 - \varepsilon^2)^2 - \right.$$

$$\left. - \frac{5}{256}(1 - \varepsilon^2)^3 + ... \right\} . \qquad (4.3.7)$$

Neglecting the third, the fourth, and higher terms, averaged value, β , becomes

$$\beta = \frac{1}{\gamma^{1/2}\, \varepsilon\, \lambda} \frac{3 + \varepsilon^2}{4} . \qquad (4.3.8)$$

Replacing the $\beta(\theta)$ in (4.3.5) with β of (4.3.8), the integration over θ can be accomplished.

$$(S.T.) = - \sqrt{\frac{2}{\pi}}\, \gamma^{1/2} \frac{\varepsilon}{(1 - \varepsilon^2)^{1/2}} L_n(\varepsilon) \left\{ 1 - \right.$$

$$\left. - \frac{\beta}{2} \left[\int_0^{\infty} (\beta^2 + x)^{1/2} \exp\left(- \frac{x}{2} \right) dx - 2\beta \right] \right\} ,$$

$$(4.3.9)$$

where $x = a (a + 2\beta)$.

The trial value $\langle E_{000} \rangle^S$, (4.3.2), becomes

$$\langle E_{000} \rangle^S = \gamma (1 + \frac{1}{4} \varepsilon^2) -$$

$$-\sqrt{\frac{2}{\pi}}\,\gamma^{1/2}\,\frac{\varepsilon}{(1-\varepsilon^2)^{1/2}}\,L_n(\varepsilon)\left\{1-\frac{\beta}{2}\right.$$

$$\left.\times\left[\int_0^{\infty}(\beta^2+x)^{1/2}\exp\left(-\frac{x}{2}\right)dx-2\beta\right]\right\}. \qquad (4.3.10)$$

Comparing (4.3.10) with (4.2.15) which is given by W-B, (4.3.10) coincides with (4.2.15) in the case of no screening, $\lambda = \infty$, (i.e. $\beta = (3+\varepsilon^2)/(4\varepsilon\gamma^{1/2}\lambda) = 0$). By the screening effect which is expressed by the term including β, the expectation value of the energy, $\langle E_{000}\rangle^s$, becomes large. Therefore the binding energy,

$$E_{000}{}^s = \gamma - \langle E_{000}\rangle^s, \qquad (4.3.11)$$

decreases by the screening effect.

The variational condition to minimize $\langle E_{000}\rangle^s$ with respect to ε was determined by the numerical method using computer and this condition was used to decide the expectation value of $\langle E_{000}\rangle^s$. The affection of screening on the binding energy, (4.3.11), is shown in Fig. 14 for several values of the screening length, λ.

Extending this method to the (110) state, we have for the trial value, $\langle E_{110}\rangle^s$,

$$\langle E_{110}\rangle^s = \gamma\left(3+\frac{1}{4}\varepsilon^2\right)-\sqrt{\frac{1}{2\pi}}\,\gamma^{1/2}\,\varepsilon\left[\frac{2-\varepsilon^2}{(1-\varepsilon^2)^{3/2}}L_n(\varepsilon)\right.$$

$$\left.-\frac{2}{1-\varepsilon^2}\right]\left[1-\left\{\frac{\beta}{4}(\beta^2+3)\int_0^{\infty}(\beta^2+x)^{1/2}\exp\left(-\frac{x}{2}\right)dx\right.\right.$$

$$\left.\left.-\frac{1}{2}\beta^2(\beta^2+4)\right\}\right]. \qquad (4.3.12)$$

(4.3.12) is equal to (4.2.18) of W-B again in the case of $\beta = 0$. The binding energy, E_{110}^{s} is

$$E_{110}^{s} = 3\gamma - \langle E_{110} \rangle^{s} \quad . \qquad (4.3.13)$$

The result of the binding energy, E_{110}^{s}, is shown in Fig. 15. Comparing the present results for E_{000}^{s} with that by Fenton and Haering, the agreement between the both results is considerably worse in the range of $\lambda^2 < 0.25$. However, in our experimental range, $\gamma < 15$, the discrepancy is within 10 %. For the each value of λ^2, the energy difference, $E_{000}^{s} - E_{110}^{s}$ is shown in Fig. 16 as a function of γ. Here the same value of 0.76 meV for 1 Ry* is also used in the calculation as in Fig.13 . The results indicate that the energy difference, $E_{000}^{s} - E_{110}^{s}$, is not varied seriously with the decrease of the each binding energy, E_{000}^{s} and E_{110}^{s}, in the range of $\lambda^2 = \infty \sim 1$ and this difference decreases rapidly when λ^2 becomes smaller than 0.5 . The present result is consistent with the result by Durkan and March[22] who calculated the screening effect of (000) and its first excited state, ($0\bar{1}0$), by somewhat different manner of variational calculation. (The binding energy of ($0\bar{1}0$) is just agreed with that of (110) as is shown by W-B.)

In Fig. 13, the energy difference $\omega_I - \omega_{ct}$ could be explained well by the theory of isolated state of impurity without screening. However from the present result the energy difference is not changed by the small screening effect, namely the strength of the screening can't be determined explicitly from the energy difference of the present optical experiment.

The screening length, λ , is given by the Thomas-Fermi expression as follows:

$$\lambda^2 = \left(\frac{\pi}{3}\right)^{1/3} \frac{1}{4\, n^{1/3}\, a_B^*} \quad , \qquad (4.3.14)$$

where n is the number of conduction electrons. For the case of $n = 10^{14}$ cm^{-3}, this expression gives $\lambda^2 = 10$, and for the case of $n = 10^{15}$ cm^{-3}, $\lambda^2 = 0.4$.

Considering the above mentioned, the present experimental results should be examined from a different angle containing the screening effect, the banding effect of the impurity state: In the case of TE 1715 (doped InSb), the resistivity drop and the separation of the absorption peaks corresponding to ω_I and $\omega_{c\uparrow}$ were observed in the range of $10.1 \sim 19.3$ KOe. This result means that in this magnetic field range the impurity state begins to separate from the conduction band. On the other hand, in low magnetic field (less than 10.1 KOe), the center of the absorption curve of TE 1715 coincides with the energy corresponding to ω_I of MO 1814 but not with the energy related to $\omega_{c\uparrow}$ as shown in Fig. 7. These facts may be interpreted as follows; when the separation of the absorption peaks is not observable, the transition realized is not so simple as that between the Landau levels of free electron. Namely, even in this case the impurity state exists below the bottom of the Landau level and takes part in the transition. The center of the impurity state of TE 1715 in this case is situated in the range that the energy difference between ω_I and $\omega_{c\uparrow}$ is not changed from the value given by the theory of isolated state of impurity, i.e., the position of the center of the impurity state should be in the

range of screening length of $\lambda^2 > 1$ in Fig. 16 even if the impurity state might be affected by the screening. From the result in Fig. 14, in the range of $\lambda^2 > 1$, the binding energy of the (000) state is known to remain in a finite value. The another fact from the present experiment is that the activation energy from the impurity state to the Landau level in low magnetic field does not exist, since the resistivity does not depend on temperature. The assumption that the screening effect is the main origin of the lack of the activation energy and the resistivity drop is failed to explain that the center of the absorption of TE 1715 in Fig. 7 is correspond to the energy related to ω_I, of MO 1814 instead of $\omega_{c\uparrow}$.

Consequently, our experimental results should be understood by other effect which is believed as a banding effect in magnetic field. In the case of doped InSb (TE 1715), the impurity state (we call this state as "impurity band") exists and continues to the bottom of the Landau level (the conduction band) in low magnetic field, and as the magnetic field strength is increased, this band suddenly splits away from the Landau level at a critical magnetic field.

In the next section, therefore, our experimental results will be examined from the view point of impurity band.

4 - 4. Impurity Band in Strong Magnetic Field

By the present optical absorption measurement, the resistivity drop of n-type InSb in magnetic field was proven to originate with a repopulation of electrons by electric field. Accordingly the non-ohmic properties of n-type InSb is explained by the two-band model proposed by Miyazawa and Ikoma. In sections 4 - 2 and 4 - 3 , the author have treated the impurity states as the isolated levels though these states should be considered to be "impurity band" , and the optical spectrum corresponding to ω_I should reflect the density of state of the impurity band.

As for the impurity band, Matsubara and Toyozawa[23] have presented a theory based on the random lattice of impurity. This problem has been extended by Yonezawa.[24] They treated the electron transfer in the random lattice by using the method of Green's function and calculated the density of state and the conductivity of the impurity band. Recently the influence of the magnetic field on these theory has been studied by Hasegawa and Nakamura[25] and Saitoh et al..[26] The theory by Hasegawa and Nakamura is based on an approximation of the strong magnetic field condition whereas that of Saitoh et al. is correct in the limit of weak magnetic field. The present experimental results should correspond to the theory by Hasegawa and Nakamura. In this section the relation of the present experimental results to their theory is discussed.

The derivation of the density of state of the impurity band from the optical spectrum was made as follows:

First, from the data of the transmission ratio in Figs. 5, 6, 7,

and 8, the absorption coeffecient was calculated. For this purpose the formula of the transmission, T, used is given by

$$T = \frac{(1 - R)^2 e^{-\alpha d}}{1 - R^2 e^{-2\alpha d}} , \qquad (4.4.1)$$

where α , d , and R are the absorption coeffecient, the thickness of sample, and reflectivity respectively. R for normal incidence is expressed as usual by

$$R = \frac{(n - 1)^2 + k^2}{(n + 1)^2 + k^2} ,$$

where n and k are the refractive index and the extinction coefficient respectively. For InSb, the dielectric constant κ is 16 , therefore $n = \sqrt{\kappa} = 4$ and k is ignored. The reflectivity, R , becomes 0.36. The ratio of the transmission in magnetic field, $T(H)$, to that in zero field, $T(0)$, is

$$\frac{T(H)}{T(0)} = \frac{1 - R^2 e^{-2\alpha_0 d}}{1 - R^2 e^{-2\alpha d}} \frac{e^{-\alpha d}}{e^{-\alpha_0 d}} \approx e^{-(\alpha - \alpha_0)d} , \qquad (4.4.2)$$

where α and α_0 are the absorption coefficients in and without magnetic field respectively. Since the two absorptions corresponding to ω_I and $\omega_{c\uparrow}$, resonate only to l.c.p. light, therefore, (4.4.2) should be rewritten as

$$\frac{T(H)}{T(0)} - \frac{1}{2} = \frac{1}{2} e^{-\Delta\alpha d} , \qquad (4.4.3)$$

where $\Delta\alpha = \alpha - \alpha_0$, $\Delta\alpha$ is the absorption coeffecient in magnetic field.

Typical result of the absorption coeffecient, $\Delta\alpha$, derived from (4.4.3) is shown in Fig. 17. As the absorption corresponding to $\omega_{c\uparrow}$ is a usual cyclotron resonant absorption, the absorption curve of the Lorentian shape may be expected, namely,

$$\alpha(\omega) = \alpha_1 \frac{\Delta\omega}{(\omega_c - \omega)^2 + (\Delta\omega)^2} \quad , \qquad (4.4.4)$$

where $2\Delta\omega$ is the half width of the absorption line and $\alpha_1 / \Delta\omega$ is the peal value. Best fittings of the peal value and the half width in (4.4.4) to the experimental results give the dashed curve for $\omega_{c\uparrow}$. Using the relation, $\Delta\omega = 1/\tau$, the relaxation time of electrons in Landau level, τ , was calculated. The Lorentzian distribution of $\omega_{c\uparrow}$ is substracted from the experimental spectrum and the remainder is determined as the absorption corresponding to ω_I . The shape of ω_I thus obtained is plotted by dashed curve in Fig. 17.

The magnetic field dependence of the half value width, $2\Delta\omega$, of the $\omega_{c\uparrow}$ and ω_I is shown in Fig. 18 for MO 1814 and TE 1715. From this result, for MO 1814 the width of $\omega_{c\uparrow}$ is almost constant and the width of ω_I decreases with the increase of magnetic field. Therefore, the impurity band of MO 1814 becomes narrower as the magnetic field becomes stronger. Contraly to this result, in the case of TE 1715 only one line was observed at about 10 KOe though the spectrum was separated to two independent lines at about 20 KOe.

To derive the density of state of the impurity band of the

(000) state from the dashed curve corresponding to ω_I in Fig. 17, there are two difficulties: (1) The spectrum corresponding to ω_I consists of the joint density of state on the (000) and (110) states. (2) The energy dependence of the transition probability between two bands is an unknown factor. Here $\Delta\alpha$ ($\hbar\omega$) in (4.4.3) is expressed for the absorption corresponding to ω_I .

$$\Delta\alpha(\hbar\omega) \propto \sum_{E_i, E_f} \rho_{000}(E_i)\, \rho_{110}(E_f)\, |P_{if}(\hbar\omega)|^2\, \delta(\hbar\omega - E_f + E_i), \qquad (4.4.5)$$

where $\rho_{000}(E)$ and $\rho_{110}(E)$ are the energy dependent state-densities on the bands of (000) and (110) respectively. $|P_{if}(\hbar\omega)|^2$ is the transition probability from the initial state in (000), E_i , to the final state in (110), E_f . From the analogy with the problem of isolated state of impurity, an approximation,

$$P_{if}(\hbar\omega) \equiv 1 \ ,$$

is used. $\rho_{110}(E_f)$ is approximated to be the similar shape with $\rho_{000}(E_i)$ and only the width of the $\rho_{110}(E_f)$ is larger than that of $\rho_{000}(E_i)$. From the result of Fig. 10, E_{110} is roughly (2/3)E_{000} . Here the following formula of the hydrogenic energy levels is used:

$$E_n = \frac{m^* e^4}{2\hbar^2 \kappa^2} \frac{1}{n^2} = \frac{\hbar^2}{2 m^*} \frac{1}{(a_B^*)_n^2} \ .$$

The dummy quantum number for the state (110), n , is $(3/2)^{1/2} = 1.22$. Therefore the state of (110) is 1.22 times wider than that of (000)

becouse $(a_B^*)_{110} \sim 1.22 (a_B^*)_{000}$. For the two gaussian states having the above relation, numerical study of (4.4.5) gives that the width of ρ_{000} is about 0.65 times of the width of the absorption spectrum of ω_I . By using these approximations, $\rho_{000}(E_i)$ can be derived from $\Delta\alpha(E)$.

Of course this procedure is the very rough approximation, but we do not have any adequate method for the derivation of the impurity band of (000) from the spectrum of ω_I .

Before carrying out this procedure to the impurity band, we study the conduction band. As is well known, the density of state of the conduction band in the case of zero magnetic field is

$$\frac{d N_0}{d E} = \left[\frac{m^{*3/2}}{\sqrt{2}\, \pi^2 \hbar^3} \right] E^{1/2} , \qquad (4.4.6)$$

where the degeneracy of spin is neglected. When the magnetic field is applied, the density of state of the lowest Landau level is

$$\frac{d N}{d E} = \left[\frac{m^{*3/2}}{\sqrt{2}\, \pi^2 \hbar^3} \right] \frac{\hbar \omega_c}{2} E_z^{-1/2} \qquad (4.4.7)$$

where E_z is the z-component of the energy. If the damping of the Landau level is concerned the energy E_z should be replaced by $E_z + i \Gamma$, where $\Gamma = 1 / \tau$. Then (4.4.7) becomes

$$\frac{d N}{d E} = \left[\frac{m^{*3/2}}{\sqrt{2}\, \pi^2 \hbar^3} \right] \frac{\hbar \omega_c}{2} \left\{ \frac{E_z + (E_z^2 + \Gamma^2)^{1/2}}{2 (E_z^2 + \Gamma^2)} \right\}^{1/2} . \qquad (4.4.8)$$

The densities of state of the impurity band and the conduction band are demonstrated in Fig. 19 by using the above relations in the case of MO 1814. The origin of the energy is always taken at the bottom of the conduction band. Using eq. (4.4.6), the density of conduction band in zero magnetic field is drawn by the thick solid curve. The density of the Landau level is reproduced from eq. (4.4.7) for each value of magnetic field. As is shown in Fig. 18, the electron of the Landau level has a finite relaxation time. Therefore using (4.4.8) in which the value of Γ is determind from the relation, 2Γ = half-value-width, the damped Landau levels are shown by dashed curves. The tails of Landau levels are penetrated to the lower side of the conduction band. The density of state of the (000) band is reproduced from the spectra of ω_I by narrowing its width by a factor of 0.65 as is mentioned before and is shown by the solid line. The position of the gravity center of the (000) band is situated at that given by Y.K.A. (cf. Fig. 10). The relative size of the impurity band to the conduction band is determined by choosing the total area of impurity band to be equal to the area of conduction band up to the Fermi level of the degenerate electrons in zero magnetic field. In Fig. 19, the shape of impurity band in zero magnetic field is roughly drawn as the dashed curve which is obtained by using the extraporated value of the line width to zero field in Fig. 18. The density of state given by Matsubara-Toyozawa, which is indicated by narrow solid curve in the same figure, corresponds to this zero field case.

Same kind of the procedure is made for the case of TE 1715 and the result is shown in Fig. 20. The results in Figs. 19 and 20 are qualitatively well agreed with the theory of the magnetic field dependence of the density of state of impurity band given by Hasegawa and Nakamura.

In comparison with the present results, the results by Hasegawa and Nakamura are shown in Fig. 21. They gave a criterion on the transition from single band phase to two-band phase in the following form:

$$f = \frac{4\pi c \hbar^2 N_D}{e H \sqrt{2 m^* E_b(H)}} = \frac{8}{27} , \qquad (4.4.9)$$

where $E_b(H)$ is the binding energy of the isolated state of impurity in magnetic field and N_D is the total donor concentration. For TE 1715 ($N_D - N_A = 1.7 \times 10^{15}$ cm^{-3}), the critical magnetic field, H , given from eq. (4.4.9) is 18.4 KOe assuming $N_A / N_D = 0.15$. Though the compensation ratio of TE 1715 is unknown the compensation is expected to be appreciably small, since the sample was prepared by doping tellurium impurity into a pure material. The agreement between the present experimental result and their theoretical value is satisfactory. There are other experimental results suggesting the separation of the impurity state from conduction band by the freeze-out effect. Frederikse and Hosler[27] and Neuringer[28] investigated the magnetic field dependence of the Hall coefficient ($R_H = 1 / N e$) of n-type InSb at low temperature and found the sharp rise of the Hall coefficient of the highly doped sample at a certain critical magnetic field. This sharp rise is considered to be originated in the decrease of the number of electrons in conduction band, N . Therefore at the magnetic field corresponding to the sharp rise of R_H , the phase of n-type InSb is transformed from single-band phase to two-band phase. Hasegawa and Nakamura have presented the phase diagram of the formation of impurity band. This diagram is shown in Fig. 22. In this figure, the present experimental result on TE 1715 and the results of Frederikse-Hosler and Neuringer

are also plotted. The agreement between experimental values and the critical value given by Hasegawa and Nakamura is satisfactory.

From the above whole discussion, it is concluded that the impurity state of n-type InSb in magnetic field forms a band and therefore the proposal by Miyazawa and Ikoma is supported.

§. 5 Conclusions

The impurity state in n-type InSb in strong magnetic fields was studied at low temperatures by means of the optical absorptions and the transport measurements. The results indicate the forming of band in the impurity states. Magnetic field dependence of the structure of the impurity band was reproduced from the optical spectrum due to the transition between associated states of impurity with Landau levels. The separation of the impurity band from the conduction band was observed in the case of the high impurity concentration as increasing the strength of magnetic field. The process of the banding is qualitatively and quantitatively well explained by the recent theory of impurity band in magnetic field.. On the origin of the non-ohmic properties in n-type InSb discussed recently by many investigators, the present experimental result supports the two-band model than the hot electron effect in the single band. The screening effect by conduction electrons on the impurity states was also studied. However the strength of the screening can not be determined explicitly from the present experimental results.

Acknowledgements

The author expresses his sincere thanks to Professor S. Narita for his continual guidance and encouragement. He would also like to thank to Dr. Y. Nishida and K. Nagasaka for their useful suggestions. Helpful discussions with the members of the laboratory of Prof. Narita are gratefully acknowledged.

References

1). R. J. Sladek, J. Phys. Chem. Solids 5, 157 (1958).

2). Lien Chih-ch'ao and D. N. Nasledov, Fiz. tverdogo Tela 2, 793 (1960). translation: Soviet Physics-Solid State 2, 729 (1960).

3). H. Miyazawa and H. Ikoma, J. Phys. Soc. Japan 23, 290 (1967), H. Miyazawa, J. Phys. Soc. Japan 26, 700 (1969).

4). W. S. Boyle and S. D. Brailsford, Phys. Rev. 107, 903 (1957).

5). R. Kaplan, Proc. Intern. Conf. Semiconductors. Kyoto, 1966 (J. Phys. Soc. Japan 21, Suppl.) p. 249.
B. D. McCombe, S. G. Bishop, and R. Kaplan, Phys. Rev. Letters 18, 748 (1967).
R. Kaplan and R. F. Wallis, Phys. Rev. Letters 20, 1499 (1968).

6). D. H. Dickey, E. J. Johnson, and D. N. Larsen, Phys. Rev. Letters 18, 599 (1967).

7). S. M. Kogan, Fiz. tverdogo Tela 4, 2474 (1962). translation: Soviet Physics - Solid State 4, 1813 (1963).

8). R. F. Kazarinov and V. G. Skobov, Zh. eksper. teor. Fiz. 42, 1047 (1962). translation: Soviet Physics - JETP 15, 726 (1962).

9). K. F. Komatsubara and E. Yamada, Phys. Rev. 144, 702 (1966).

10). R. J. Phelan, Jr. and W. F. Love, Phys. Rev. 133, A1134 (1964).

11). E. Yamada and T. Kurosawa, Proc. Intern. Conf. Semiconductors. Moscow, 1968 p. 805.

12). Y. Oka, K. Nagasaka, and S. Narita, Japan. J. appl. Phys. 7, 611 (1968).

13). R. F. Wallis and H. J. Bowlden, J. Phys. Chem. Solids 7, 78 (1958).

14). H. Hasegawa and R. E. Howard, J. Phys. Chem. Solids 21, 179 (1961).

15). G. D. Mahan and J. W. Conley, Appl. Phys. Letters 11, 29 (1967).

16). E. O. Kane, J. Phys. Chem. Solids 1, 249 (1957).

17). J. Yamamoto, H. Yoshinaga, and S. Kon, Japan. J. appl. Phys. 8, 242 (1969).

18). Y. Yafet, R. W. Keyes, and E. N. Adams, J. Phys. Chem. Solids 1, 137 (1956).

19). D. M. Larsen, J. Phys. Chem. Solids 29, 271 (1968).

20). R. Kaplan, Phys. Rev. 181, 1154 (1969).

21). E. W. Fenton and R. R. Haering, Phys. Rev. 159, 593 (1967).

22). J. Durkan and N. H. March, J. Phys. C. (Proc. Phys. Soc.) 1, 1118 (1968).

23). T. Matsubara and Y. Toyozawa, Prog. Theor. Phys. 26, 739 (1961).

24). F. Yonezawa, Prog. Theor. Phys. 31, 357 (1964).
F. Yonezawa and T. Matsubara, Prog. Theor. Phys. 35, 357 (1966).
F. Yonezawa, Prog. Theor. Phys. 40, 734 (1968).

25). H. Hasegawa and M. Nakamura, J. Phys. Soc. Japan 26, 1362 (1969), and Proc. Intern. Conf. Semiconductors. Moscow, 1968 p.1286.
M. Nakamura and H. Hasegawa, J. Phys. Soc. Japan 25, 636 (1968).

26). M, Saitoh, H. Fukuyama, Y. Uemura, and H. Shiba, J. Phys. Soc. Japan 27, 26 (1969).

27). H. P. R. Frederikse and W. R. Hosler, Phys. Rev. 108, 1136 (1957).

28). L. J. Neuringer, Proc. Intern. Conf. Semiconductors. Moscow, 1968 p. 715.

Table 1.

Sample No.	$N_D - N_A$ (cm^{-3})	Mobility at 77 ^oK (cm^2 / volt.sec.)	
TE 7512	7.5×10^{12}		undoped
MO 1814	1.8×10^{14}	6.3×10^5	undoped
TE 1715	1.7×10^{15}		Te-doped

Fig. 1

Schematic diagram of the light pipe system.
The lower part of the light pipe system is immersed in liq. He. Magnetic fields are produced by a persistent current in superconducting magnet.

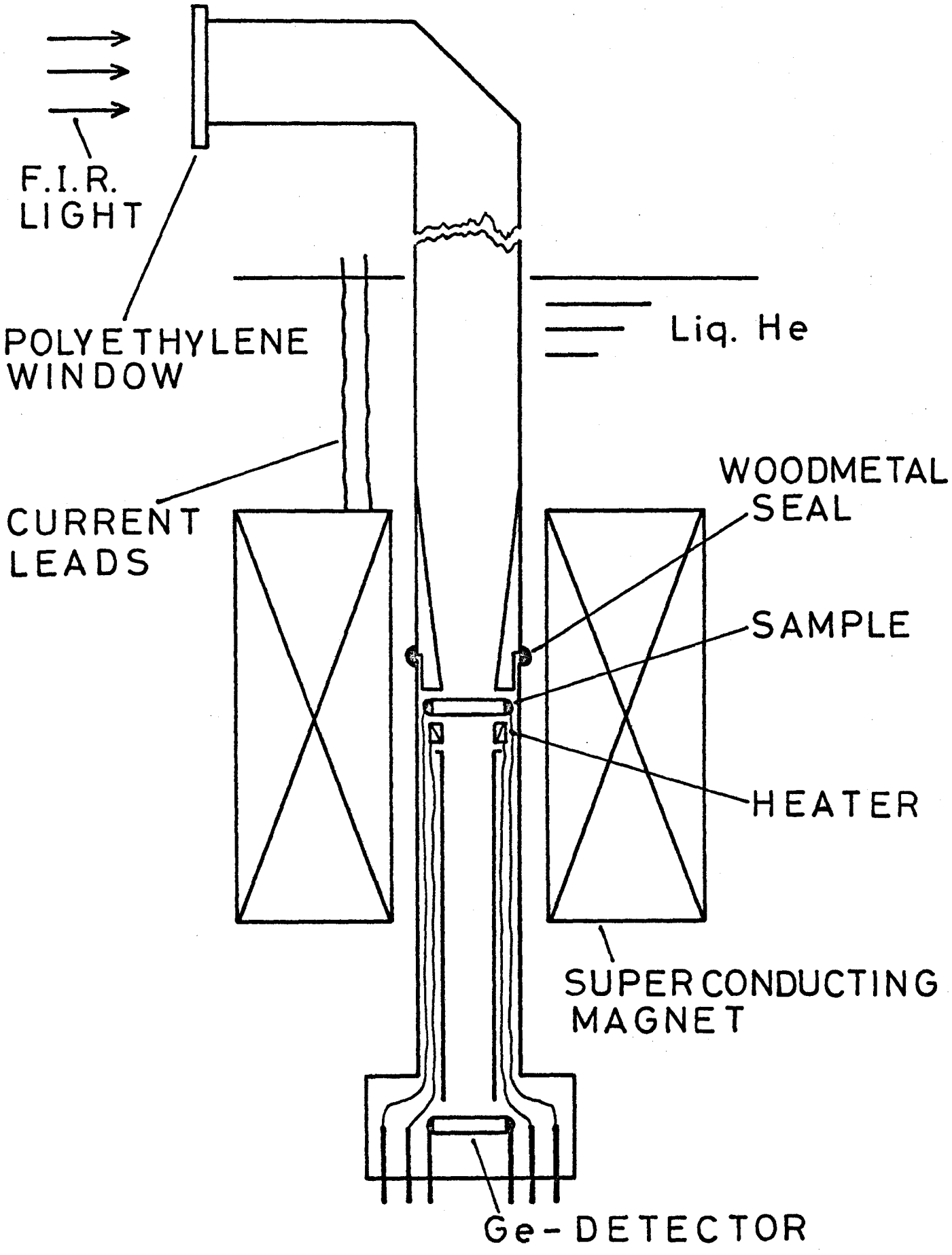
F.I.R.
LIGHT
POLYETHYLENE
WINDOW
Liq. He
CURRENT
LEADS
WOODMETAL
SEAL
SAMPLE
HEATER
SUPERCONDUCTING
MAGNET
Ge-DETECTOR

Fig. 1

Fig. 2

Schmatic diagram of the Landau levels and the impurity states of n-type InSb. The observed transitions are indicated by the arrows, where $\omega_{c\uparrow}$ and $\omega_{c\downarrow}$ are the free electron cyclotron resonant transition and ω_I is the transition between the impurity states.

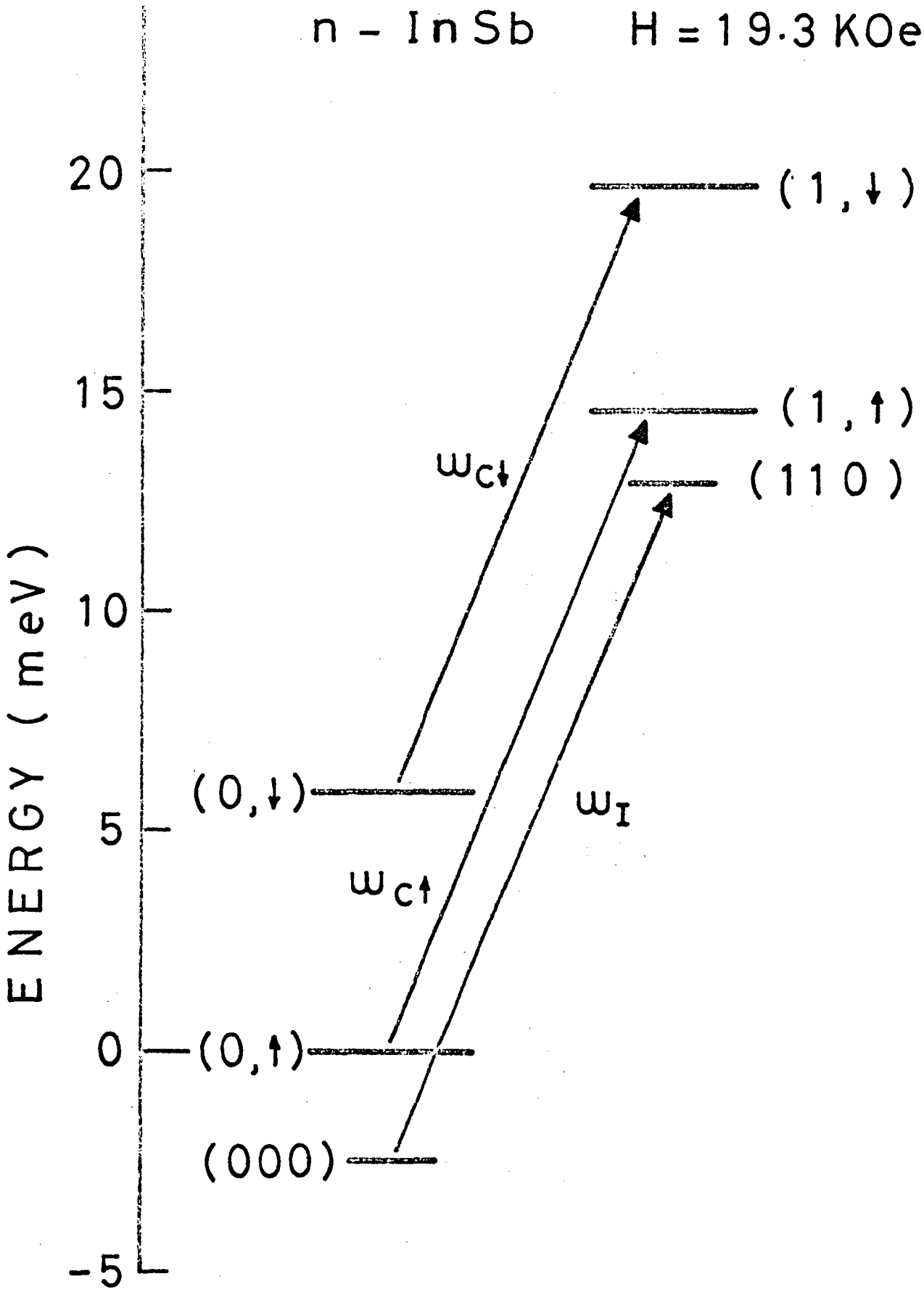

Fig. 2

Fig. 3

Electric field dependedependence of the resistivity in transverse magnetic fields and in zero magnetic field at 4.2 ^{o}K and 1.8 ^{o}K for MO 1814 ($N_D - N_A = 1.8 \times 10^{14}$ cm^{-3}).

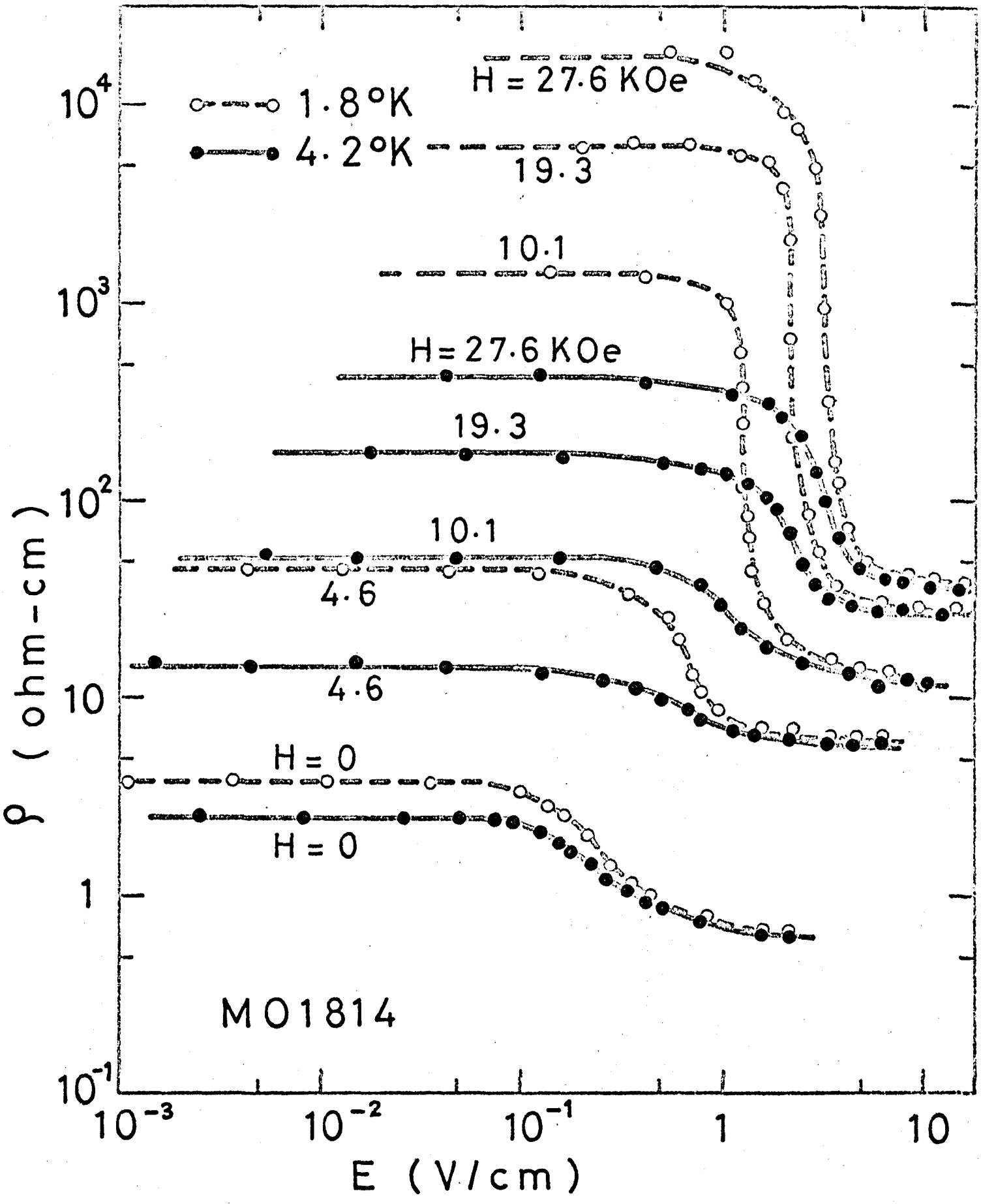
1.8°K
4.2°K
H = 27.6 KOe
19.3
10.1
H = 27.6 KOe
19.3
10.1
4.6
4.6
H = 0
H = 0
M01814
ρ (ohm-cm)
E (V/cm)
10^4
10^3
10^2
10
1
10^-1
10^-3
10^-2
10^-1
1
10

Fig. 3

Fig. 4

Electric field dependence of the resistivity in transverse magnetic fields and in zero magnetic field at 4.2 ^{o}K and 1.8 ^{o}K for TE 1715 ($N_D - N_A = 1.7 \times 10^{15}$ cm^{-3}).

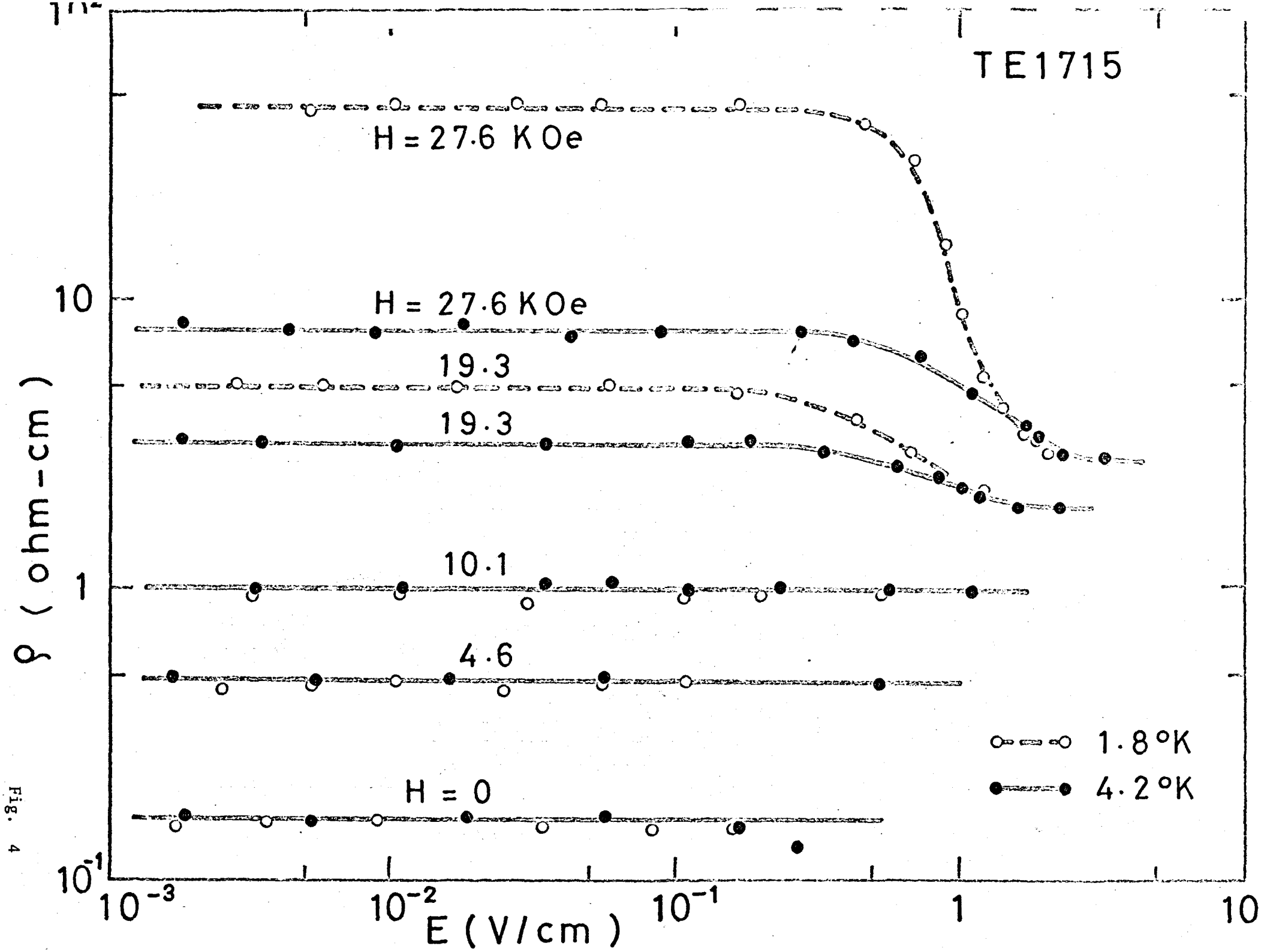
TE1715
H = 27.6 KOe
H = 27.6 KOe
19.3
19.3
10.1
4.6
H = 0
1.8°K
4.2°K
ρ (ohm-cm)
E (V/cm)
10
1
10^{-1}
10^{-3}
10^{-2}
10^{-1}
1
10

Fig. 4

Fig. 5

Transmission ratio, T(H)/T(0), as a function of wave number for MO 1814 at 1.8 ^{o}K and at 4.6 KOe. Solid curve represents the case without applying electric field and dashed curve represents the case with applying electric field of 0.77 V/cm, which is transverse to the magnetic field. Each minimum point corresponds to the energy of ω_I or $\omega_{c\uparrow}$.

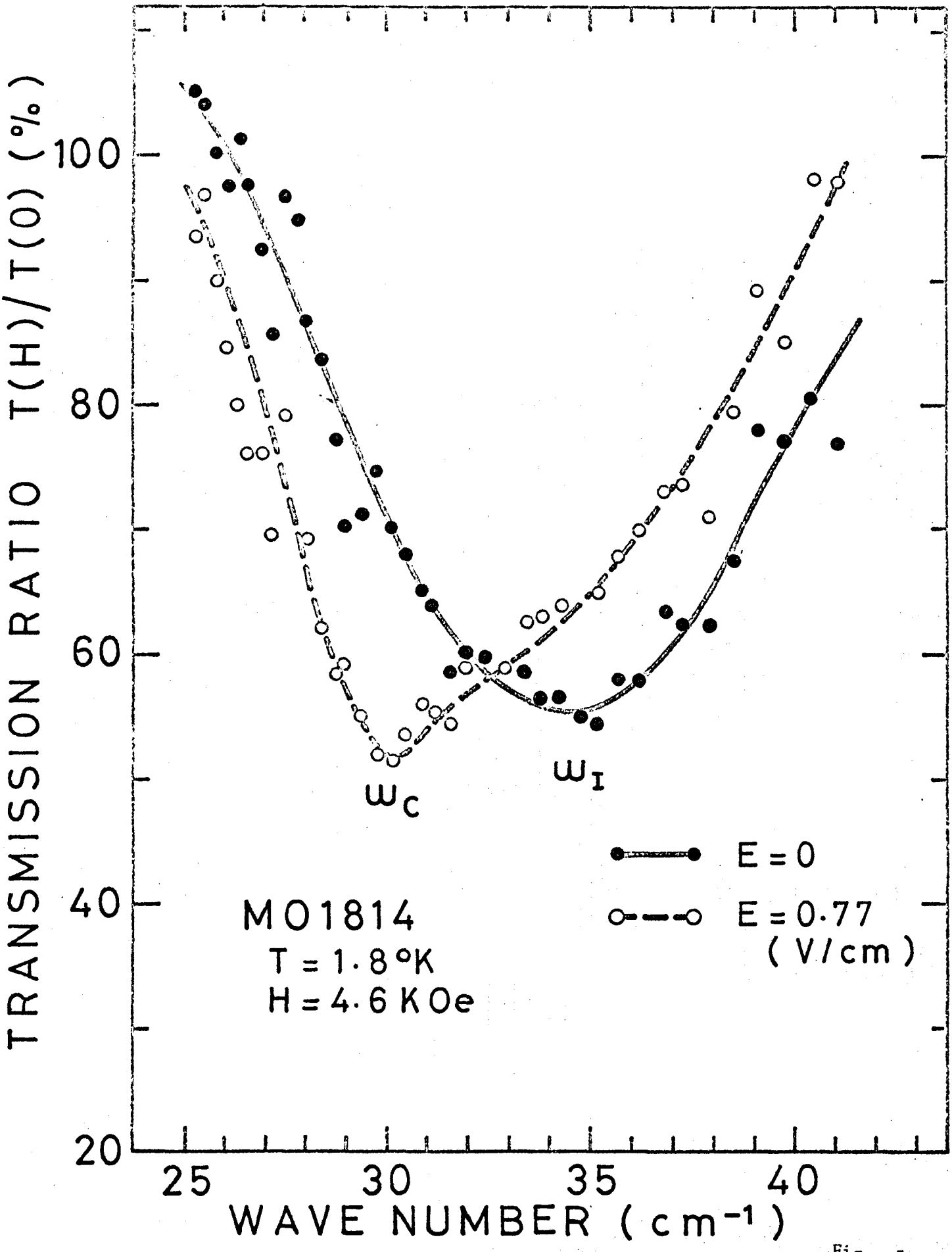
TRANSMISSION RATIO T(H)/T(0) (%)
100
80
60
40
20
25
30
35
40
WAVE NUMBER (cm⁻¹)
ωc
ωI
E = 0
E = 0·77
(V/cm)
M01814
T = 1·8 °K
H = 4·6 KOe

Fig. 5

Fig. 6

Transmission ratio, T(H)/T(0), as a function of wave number for MO 1814 at three different electric field strengths of 0, 3.9, and 6.0 V/cm, at 4.2 ^{o}K and at 19.3 KOe. At 6.0 V/cm, three transitions, ω_I , $\omega_{c\uparrow}$, and $\omega_{c\downarrow}$ are simultaneously observed.

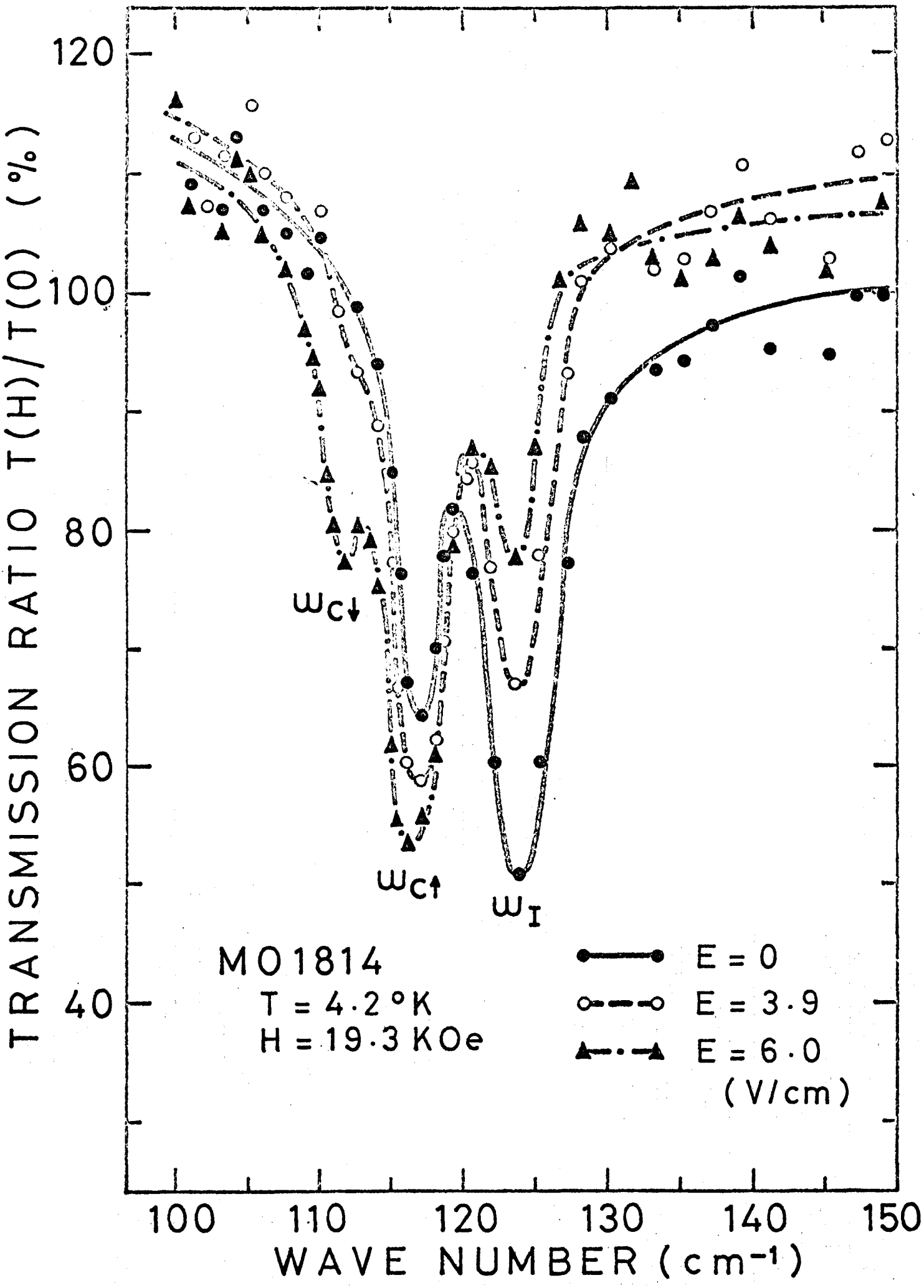
TRANSMISSION RATIO T(H)/T(0) (%)
120
100
80
60
40
100
110
120
130
140
150
WAVE NUMBER (cm⁻¹)
ωc↓
ωc↑
ωI
M01814
T = 4.2 °K
H = 19.3 KOe
E = 0
E = 3.9
E = 6.0
(V/cm)

Fig. 6

Fig. 7

Transmission ratio, T(H)/T(0) , as a function of wave number for TE 1715 with and without electric field at 1.8 ^{o}K and at 10.1 KOe. Narrow dashed curve indicates the spectra for MO 1814 at the same temperature and magnetic field and at E = 0.66 V/cm.

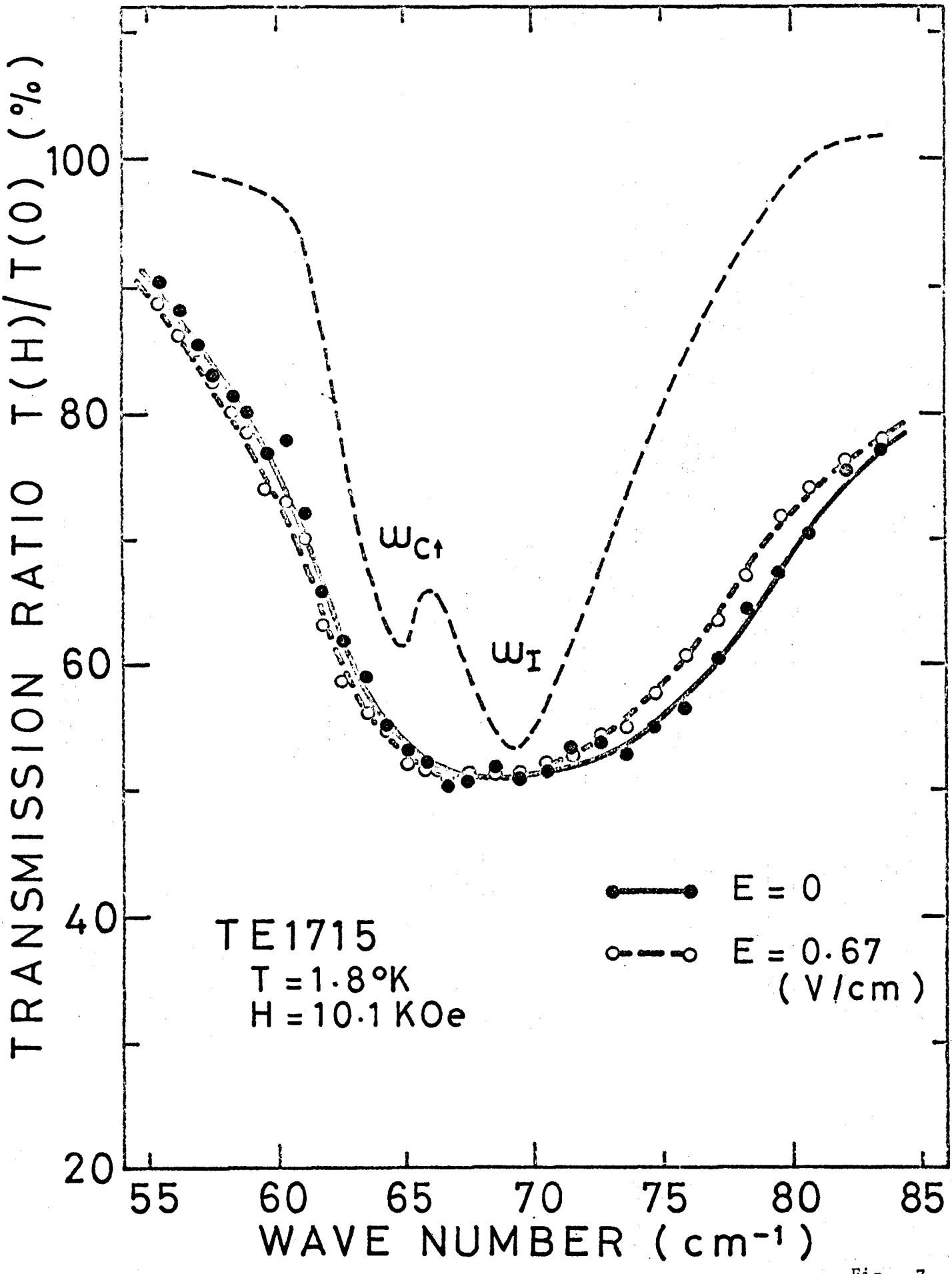
TRANSMISSION RATIO T(H)/T(0) (%)
100
80
60
40
20
55
60
65
70
75
80
85
WAVE NUMBER (cm⁻¹)
ω_C↑
ω_I
E = 0
E = 0.67
(V/cm)
TE1715
T = 1.8°K
H = 10.1 KOe

Fig. 7

Fig. 8

Transmission tatio, T(H)/T(0) , as a function of wave number for TE 1715 at 1.8 ^{o}K and at 19.3 KOe. Solid curve (E = 0 V/cm) has a remarkable shoulder at the lower wave number side, and this curve can be separated to two transmission curves correspond to $\omega_{c\uparrow}$ and ω_{I} shown by narrow dashed curves. At E = 1.17 V/cm, which corresponds to the case after resistivity drop, the intinsities of two absorptions interchange.

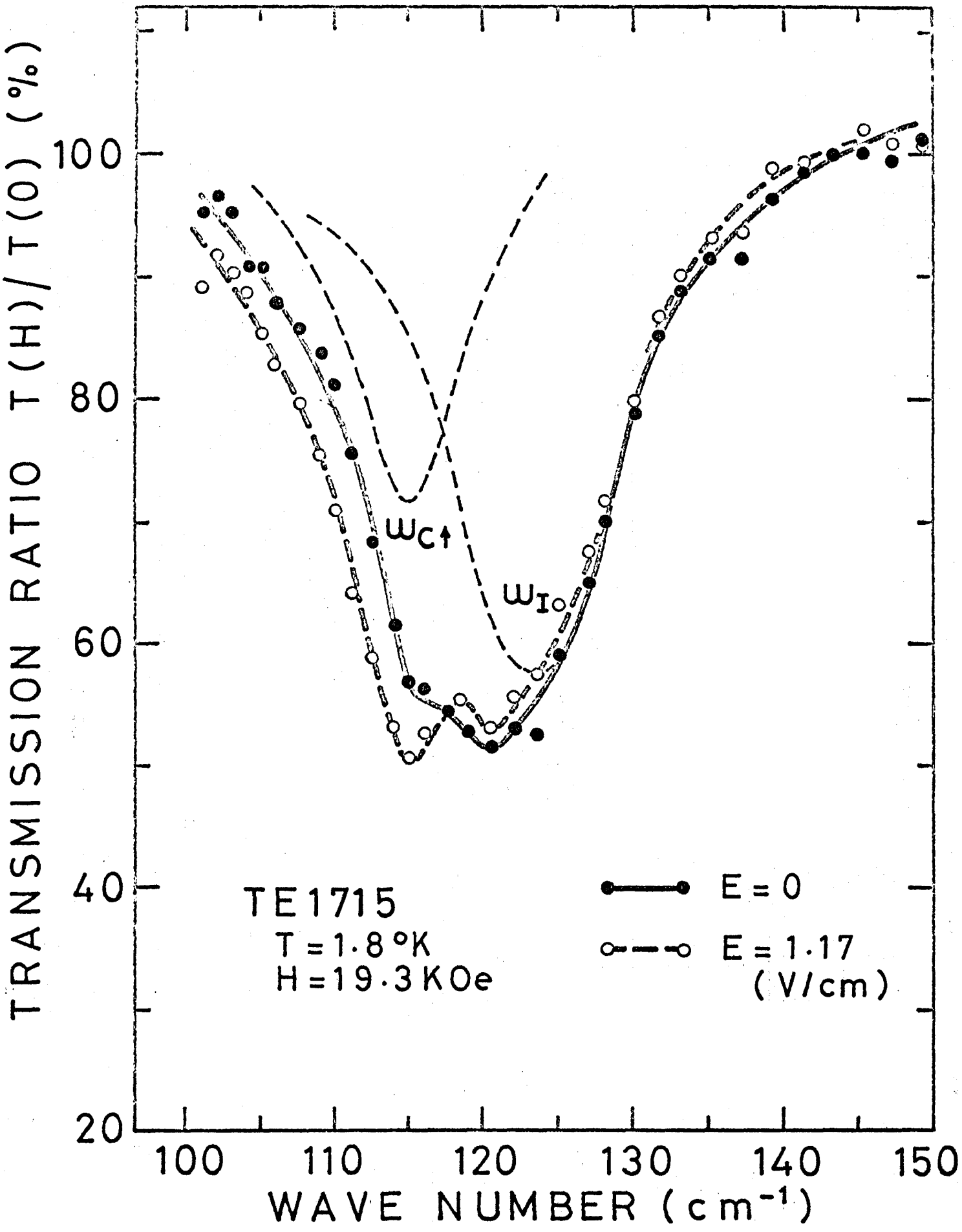
TRANSMISSION RATIO T(H)/T(0) (%)
100
80
60
40
20
100
110
120
130
140
150
WAVE NUMBER (cm⁻¹)
ωC↑
ωI○
TE1715
T = 1.8 °K
H = 19.3 KOe
E = 0
E = 1.17
(V/cm)

Fig. 8

Fig. 9

Magnetic field dependence of transition wave number ($\omega_{c\uparrow}$, $\omega_{c\uparrow}$, and ω_I) for the two samples. Effective mass of the electron was derived from the linear part of $\omega_{c\uparrow}$ curve and was $0.0143\ m_o$.

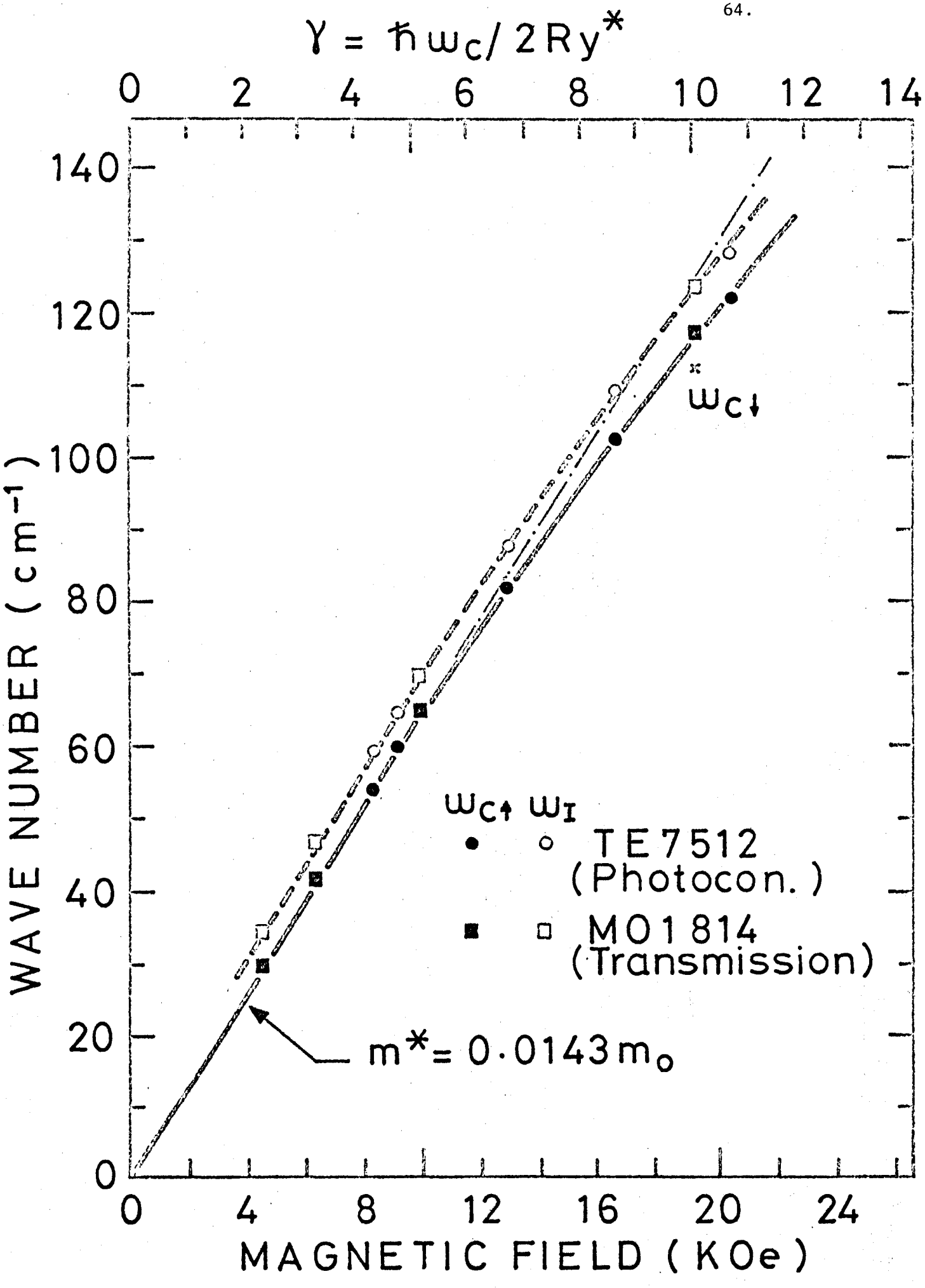
γ = ħωc/2Ry*
0
2
4
6
8
10
12
14
140
120
100
80
60
40
20
0
WAVE NUMBER (cm⁻¹)
ωc↓
ωc↑ ωI
TE7512
(Photocon.)
M01814
(Transmission)
m*= 0.0143 mo
0
4
8
12
16
20
24
MAGNETIC FIELD (KOe)

Fig. 9

Fig. 10

Binding energies of electron in (000) and (110) states, E_{000} and E_{110} , as functions of γ ($= \hbar \omega_c / 2$ Ry*) calculated by two methods. The values obtained by using one variational parameter (Wallis- Bowlden) are shown by the dashed curves and the values by two variational parameters are indicated by solid curves.

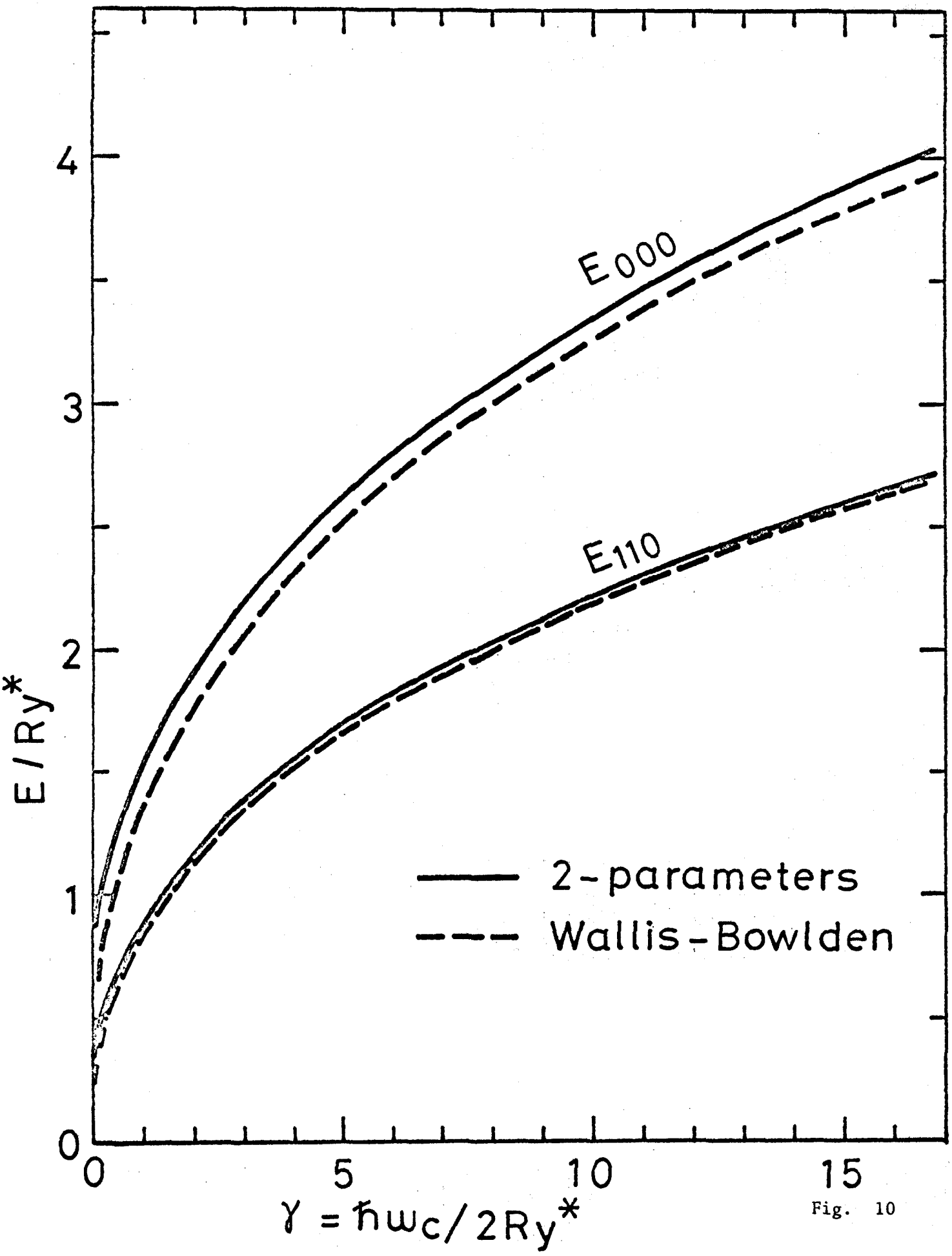
E000
E110
2-parameters
Wallis-Bowlden
E/Ry*
γ = ħωc/2Ry*
0
1
2
3
4
0
5
10
15

Fig. 10

Fig. 11

Expectation values of the orbits for (110) state; transverse orbit, $\langle a_\perp \rangle$, and parallel orbit, $\langle a_{\parallel} \rangle$, to the magnetic field, and that of free electron cyclotron orbit, ℓ_c , as functions of γ . The expectation values of each orbit is defined by $\langle a_i \rangle = \int \Psi_{110}^* \, a_i \, \Psi_{110} \, d\tau$. The relations of the expectation values to the best values of the variational parameters ($a_\perp$ and $a_{\parallel}$) and γ as follows :

$$\langle a_\perp \rangle = 2 a_\perp \quad , \quad \langle a_{\parallel} \rangle = a_{\parallel} = a_\perp / \varepsilon \quad ,$$

$$\text{and} \quad \langle \ell_c \rangle = 2 (1 / \gamma)^{1/2} \quad .$$

At the limit of $\gamma = 0$, the value of $a_\perp$ tends to $\sqrt{2\pi}$ (15/16). In this condition the value of E_{110} is $32/45\pi \sim 0.226$ in the unit of effective Rydberg, Ry* . True value of E_{110} at $\gamma = 0$ is 0.25 .

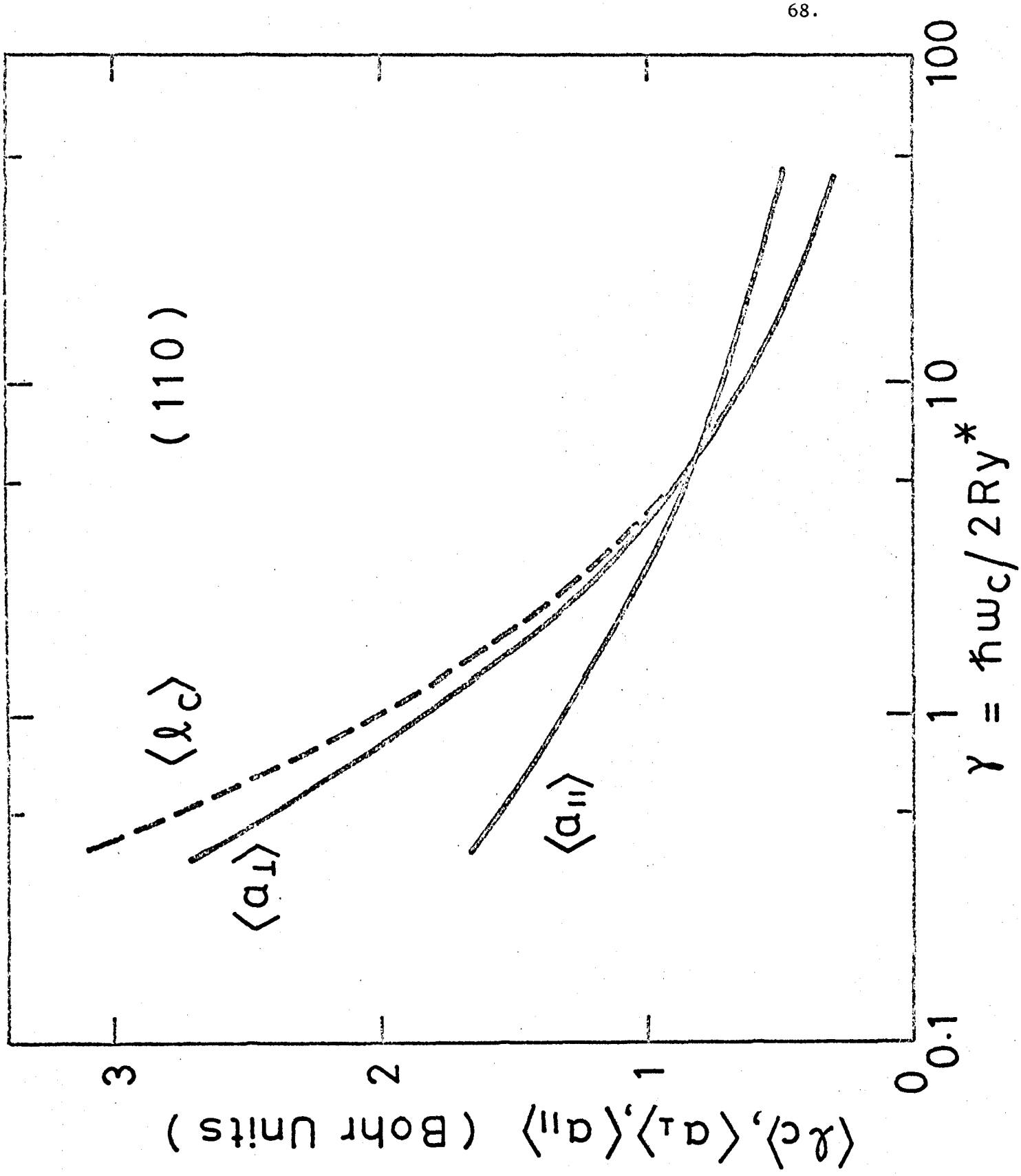

Fig. 11

Fig. 12

Expectation values of the orbits for (000) state; This figure was reperted for the first time by Y.K.A. (cf. Fig. 2 in their paper[18]). Here we also show for the comparison with Fig. 11. Expectation values are related to the variational parameters as follows :

$$\langle a_{\perp} \rangle = a_{\perp} \ , \ \langle a_{\parallel} \rangle = a_{\parallel} = a_{\perp} / \varepsilon \quad .$$

and $\langle \ell_c \rangle = (2 / \gamma)^{1/2}$.

Fig. 12

Fig. 13

Comparison of the energy difference of the present experimental values, $\hbar\omega_I - \hbar\omega_{c\uparrow}$, with the three theoretical values, $E_{000} - E_{110}$, as functions of magnetic field.

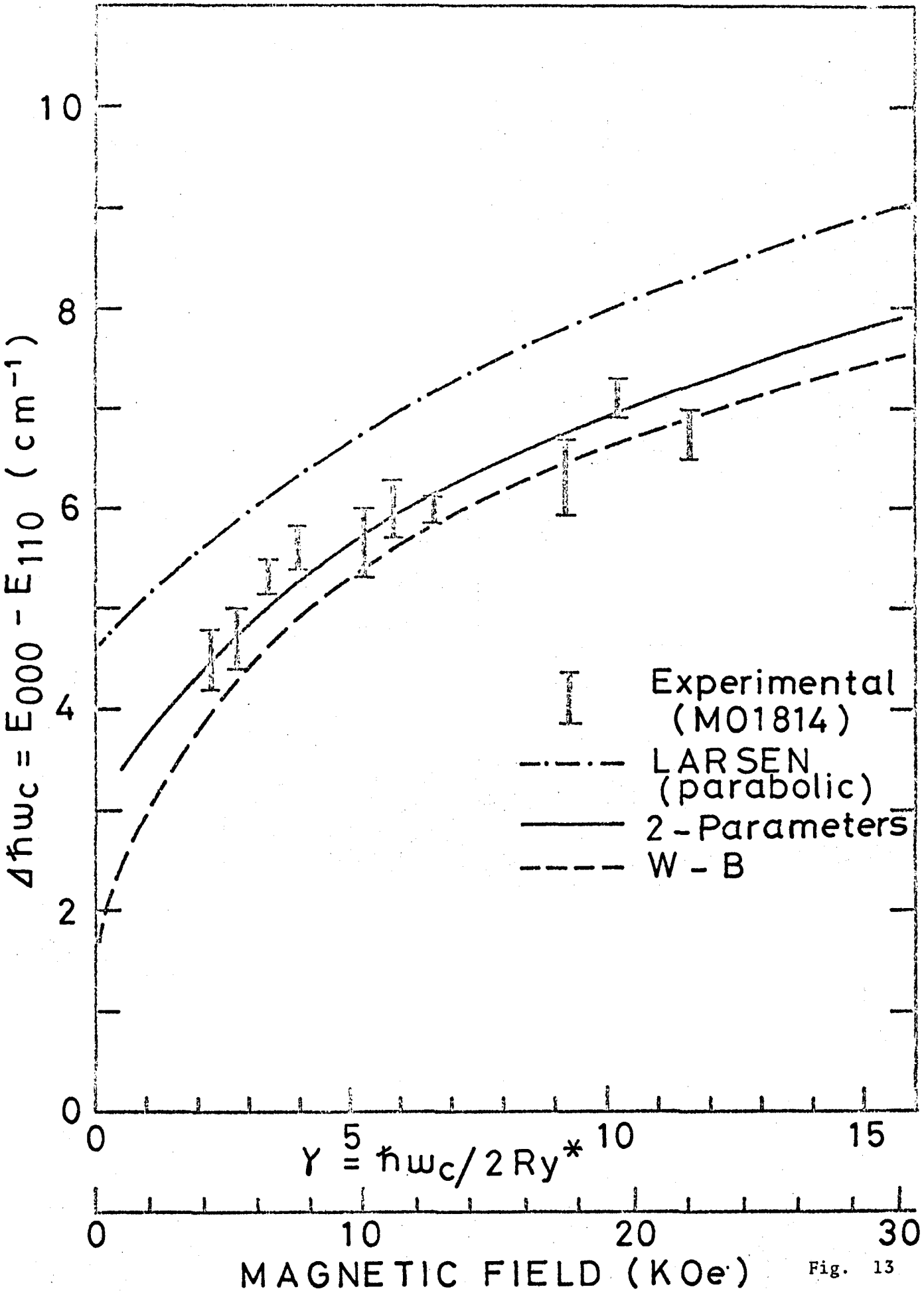
10
8
6
4
2
0
$\Delta\hbar\omega_c = E_{000} - E_{110}$ (cm^{-1})
Experimental
(M01814)
LARSEN
(parabolic)
2-Parameters
W-B
0
5
10
15
$\gamma \equiv \hbar\omega_c / 2Ry^*$
0
10
20
30
MAGNETIC FIELD (KOe)

Fig. 13

Fig. 14

Screening effect by conduction electrons on the binding energy of the (000) state, E_{000}^{s} . λ is the screening length of the impurity potential in effective Bohr units.

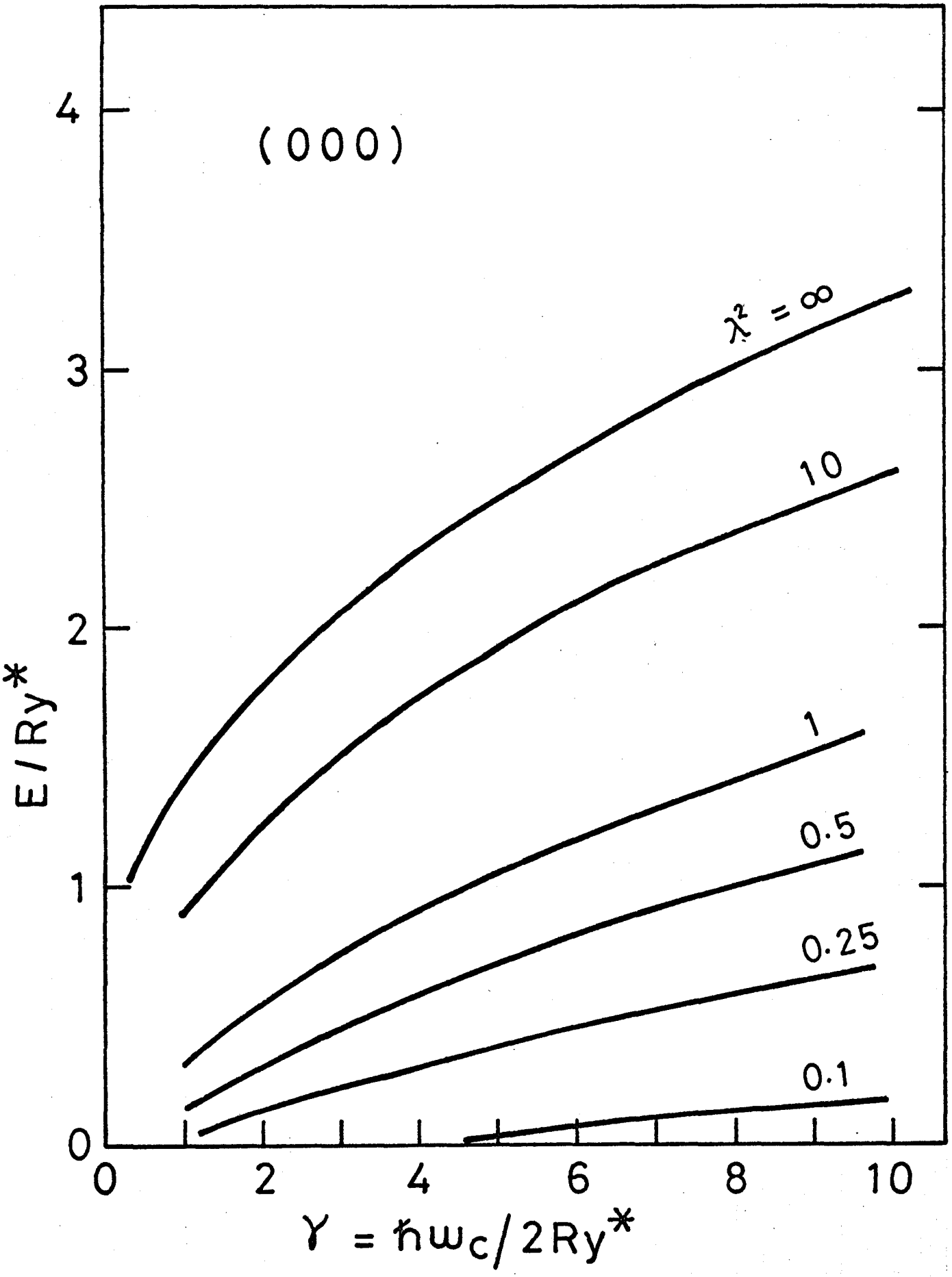
(000)
$\lambda^2 = \infty$
10
1
0.5
0.25
0.1
E/Ry*
$\gamma = \hbar\omega_c/2Ry^*$
0
1
2
3
4
0
2
4
6
8
10

Fig. 14

Fig. 15

Screening effect by conduction electrons on the binding energy of the (110) state, E_{110}^{s} .

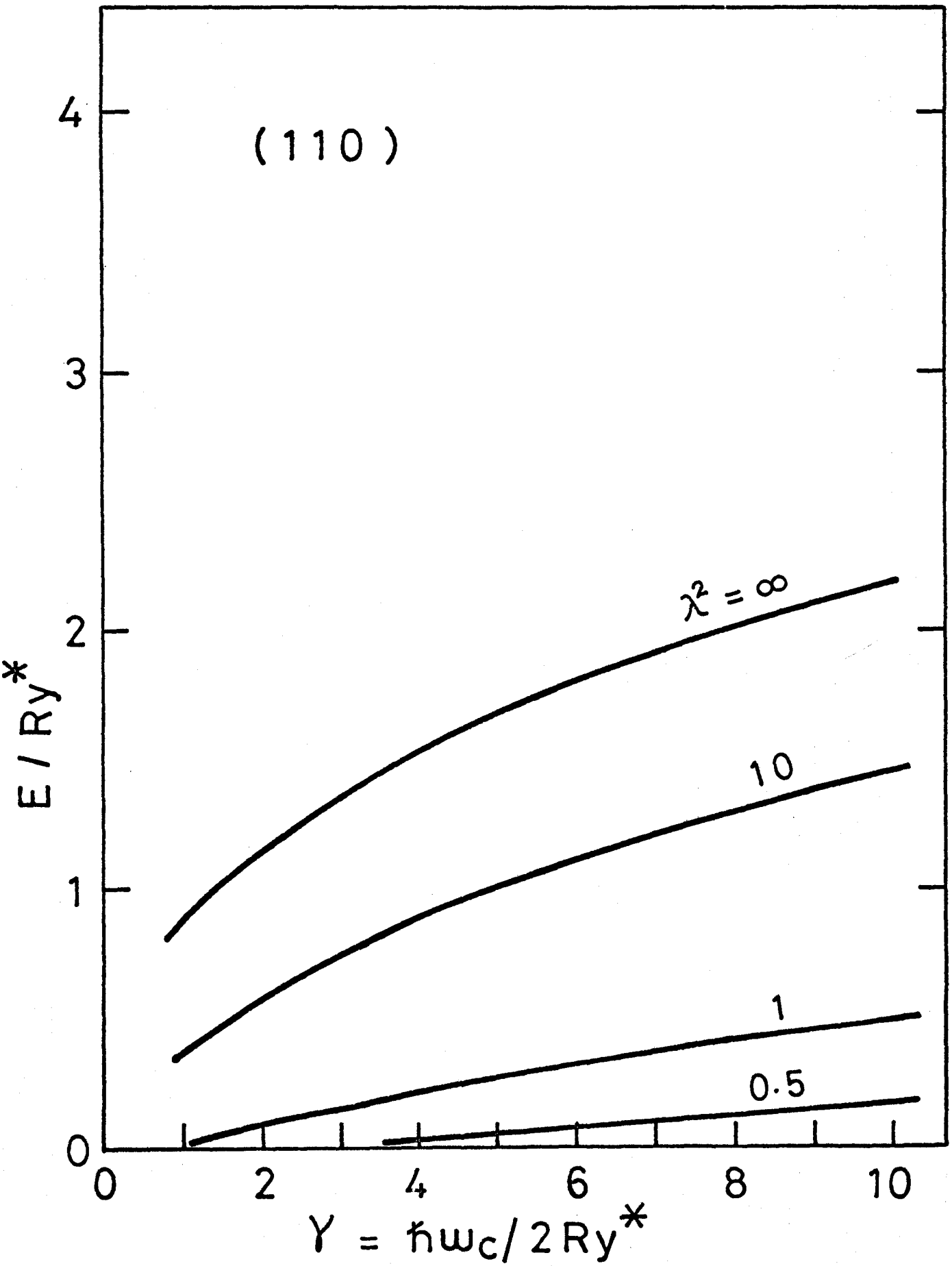
(110)
$\lambda^2 = \infty$
10
1
0.5
E / Ry*
$\gamma = \hbar\omega_c / 2Ry^*$
0
1
2
3
4
0
2
4
6
8
10

Fig. 15

Fig. 16

The affection of the screening on the energy difference between binding energies of (000) and (110), $E_{000}^{s} - E_{110}^{s}$. This figure is compared with Fig. 13 which is the case of no screening.

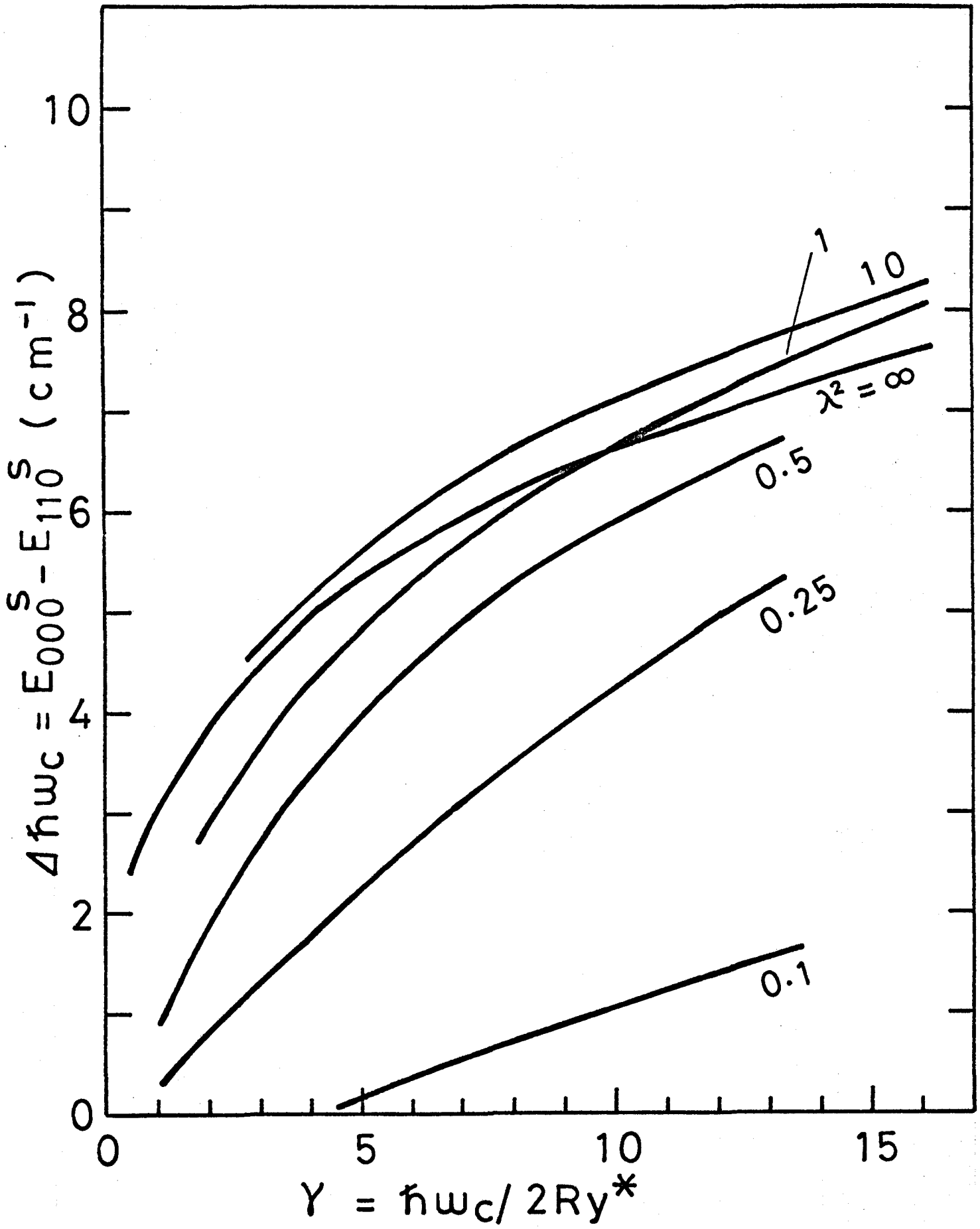
10
8
6
4
2
0
0
5
10
15
$\Delta\hbar\omega_c = E^S_{000} - E^S_{110}$ (cm^{-1})
$\gamma = \hbar\omega_c / 2Ry^*$
1
10
$\lambda^2 = \infty$
0.5
0.25
0.1

Fig. 16

Fig. 17

Absorption coefficient of the two transitions ω_I and $\omega_{c\uparrow}$ in the case of MO 1814 at 19.3 KOe and at 4.2 ^{o}K . Electric field applied is 2.6 V/cm. From the spectrum of ω_I , the shape of the impurity band is reproduced.

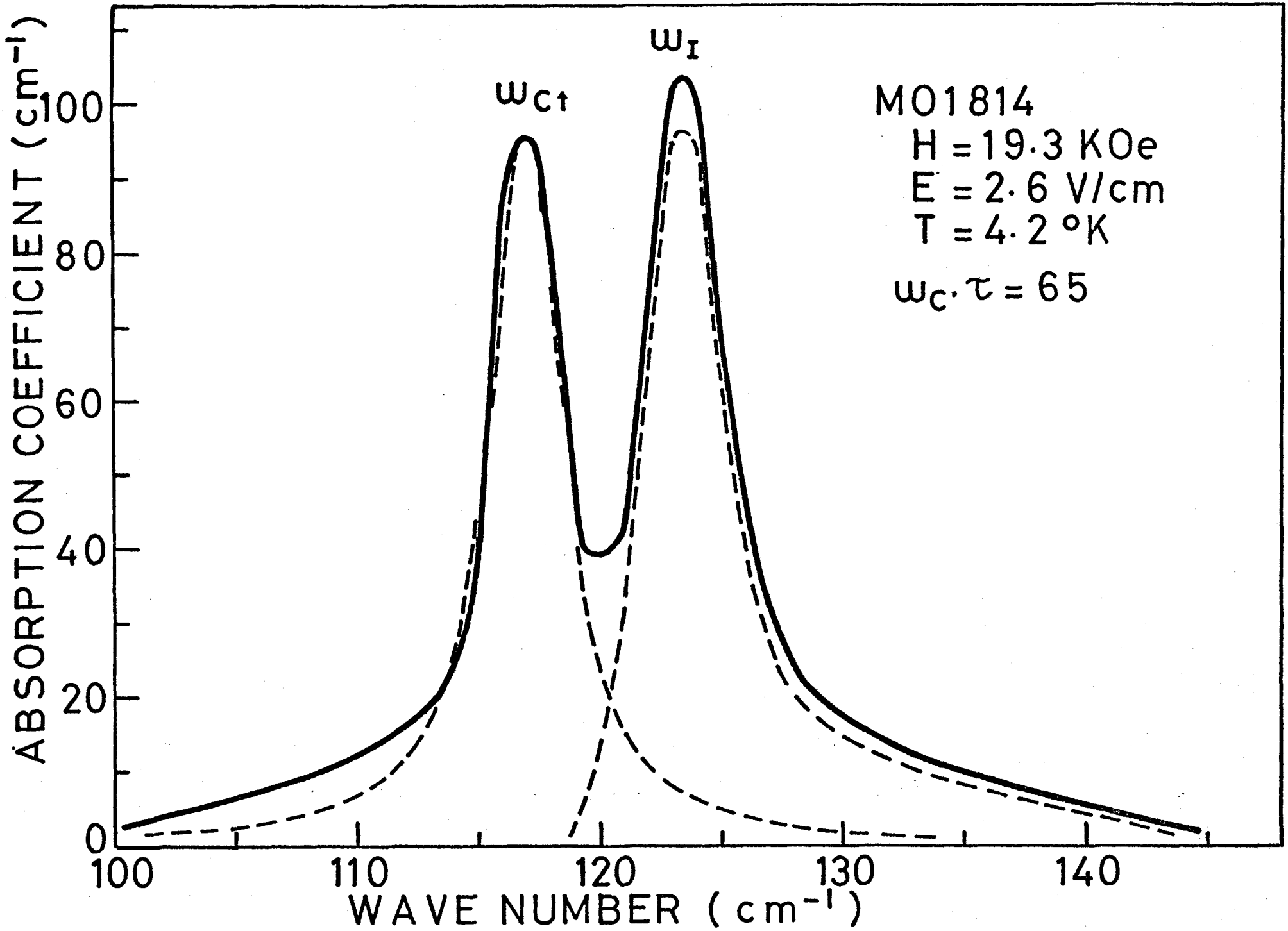
ABSORPTION COEFFICIENT (cm⁻¹)
WAVE NUMBER (cm⁻¹)
ωc1
ωI
M01814
H = 19·3 KOe
E = 2·6 V/cm
T = 4·2 °K
ωc·τ = 65
0
20
40
60
80
100
100
110
120
130
140

Fig. 17

Fig. 18

Magnetic field dependence of the line width of the spectra corresponding to ω_I and $\omega_{c\uparrow}$ for MO 1814 and TE 1715.

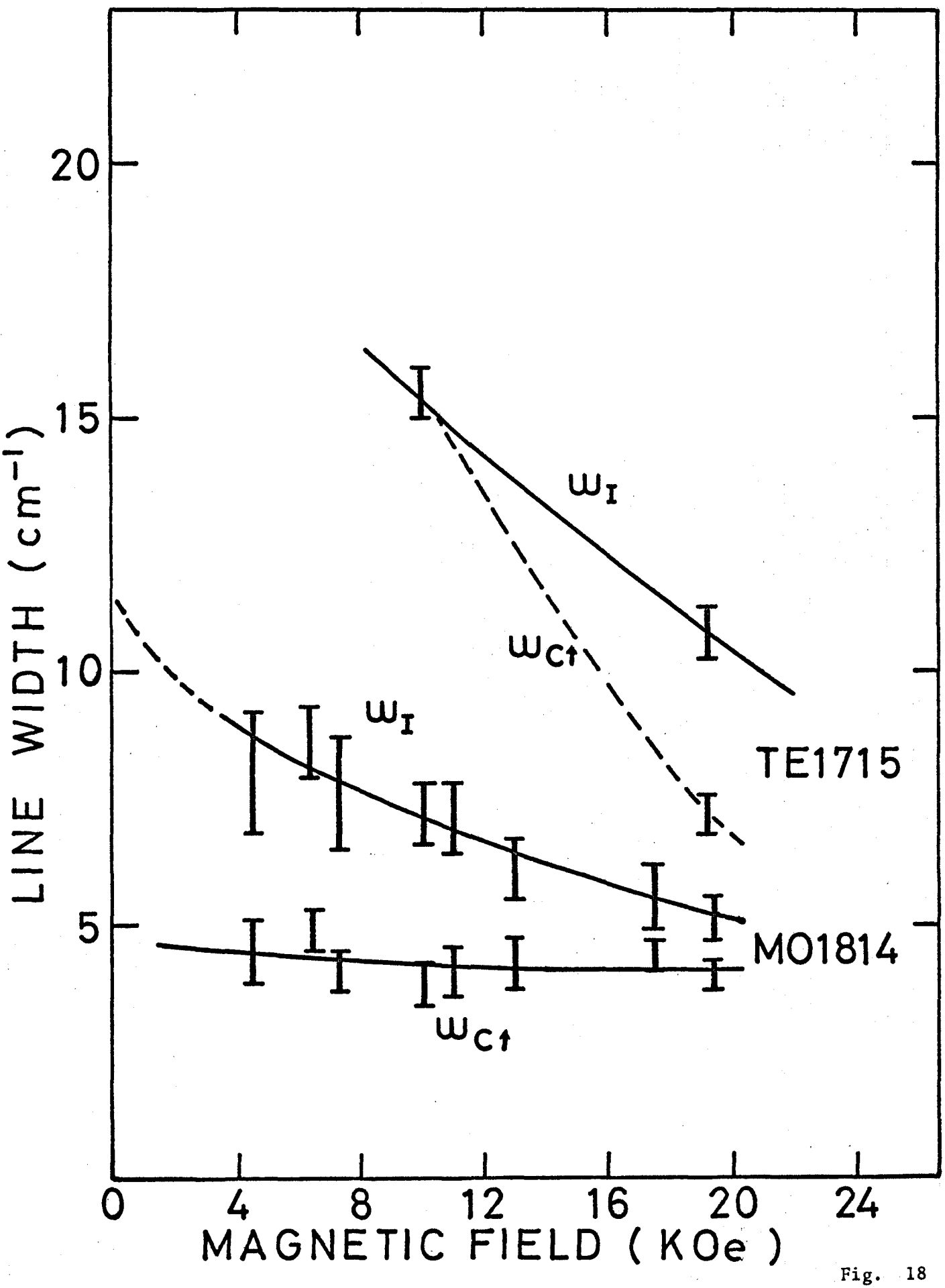
LINE WIDTH (cm⁻¹)
20
15
10
5
0
4
8
12
16
20
24
MAGNETIC FIELD (KOe)
ωI
ωCf
ωI
ωCf
TE1715
MO1814

Fig. 18

Fig. 19

Density of state of the impurity band reproduced from the optical spectrum in the case of MO 1814 is shown by the thick solid line in the negative side of the horizontal scale for two values of the magnetic field, 4.6 KOe and 19.3 KOe. The Landau levels and conduction band at zero magnetic field are also shown to compare with impurity band. The shape of impurity band in zero magnetic field is roughly drawn by dashed line by using only the extraporated value of the line width to zero field. Theoretical curve corresponding to this band is drawn by narrow solid curve from the results of Matsubara and Toyozawa. $p = 4$ in their notation means the donor concentration of 1.5×10^{14} cm^{-3} and F.L. means the Fermi level of the electron in impurity band. For the degenerate electrons in conduction band at zero magnetic field, Fermi level in the case of MO 1814 is 6.5 cm^{-1} (9.4 ^{o}K) measured from the bottom of the conduction band.

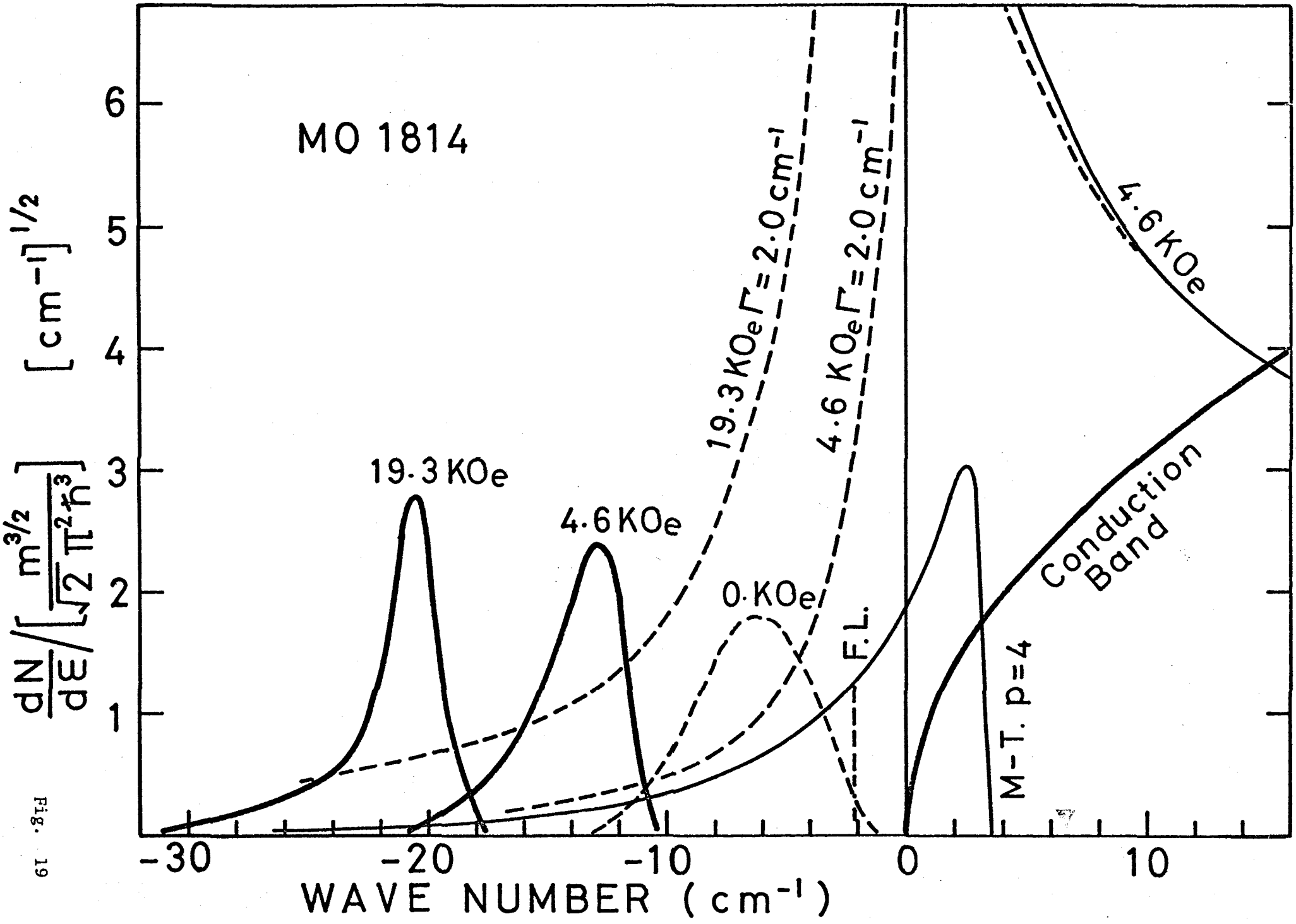
MO 1814
19.3 KOe
4.6 KOe
0 KOe
19.3 KOe Γ = 2.0 cm⁻¹
4.6 KOe Γ = 2.0 cm⁻¹
4.6 KOe
F.L.
M-T. p=4
Conduction Band
dN/dE / [m^3/2 / √2 π² ħ³] [cm⁻¹]^1/2
WAVE NUMBER (cm⁻¹)
-30
-20
-10
0
10
1
2
3
4
5
6

Fig. 19

Fig. 20

Density of state of impurity band and conduction band in the case of TE 1715. At 10.1 KOe the phase of band should be single and at 19.7 KOe the phase should be two-band phase as is confirmed from the present experiment. Fermi level of degenerate conduction electrons is 29.0 cm^{-1} (42 ^{o}K) from the bottom of the conduction band.

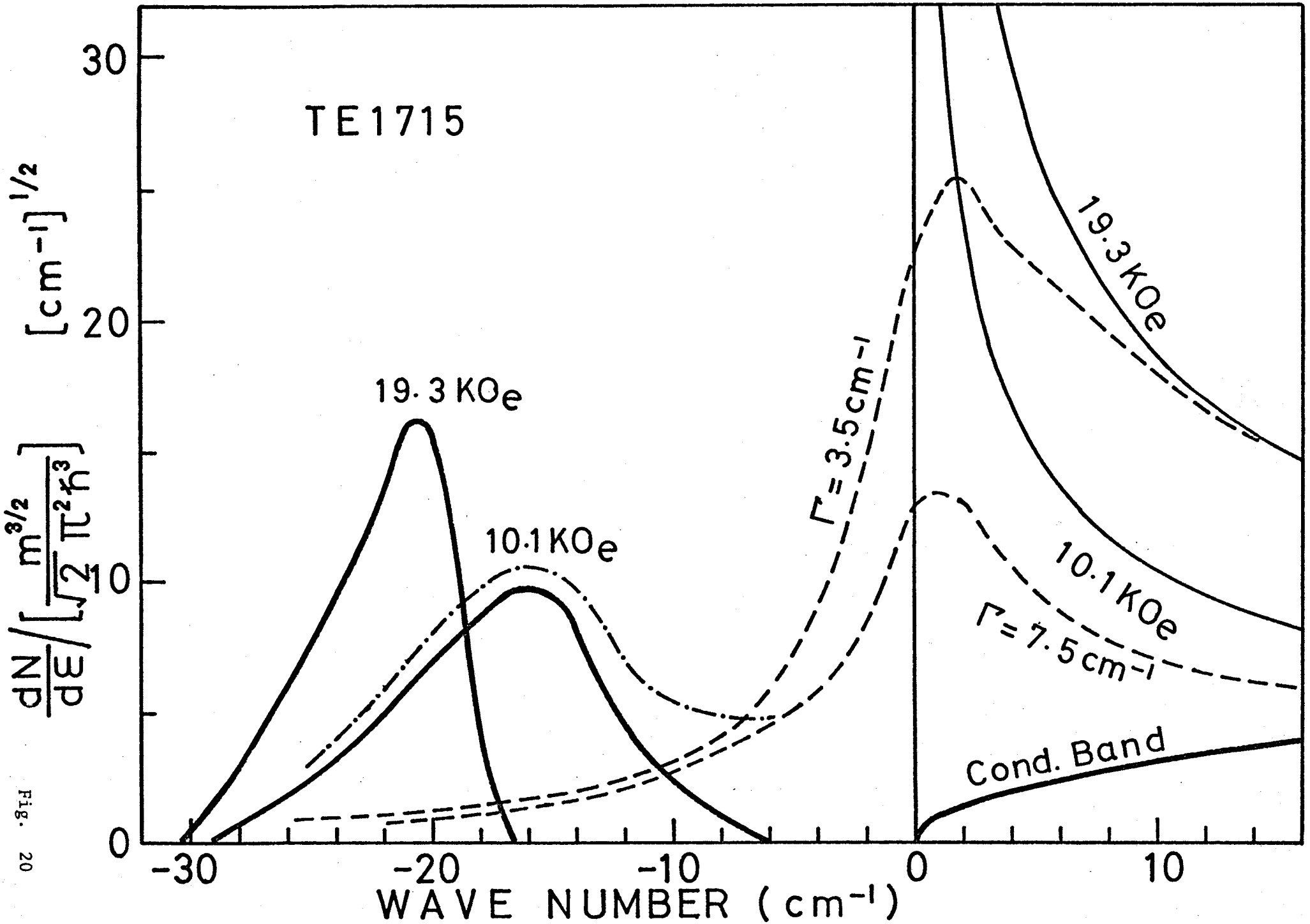
TE1715
30
20
10
0
-30
-20
-10
0
10
WAVE NUMBER (cm⁻¹)
dN/dE / [m^3/2 / √2 π²ħ³] [cm⁻¹]^1/2
19.3 KOe
10.1 KOe
Γ = 3.5 cm⁻¹
19.3 KOe
10.1 KOe
Γ = 7.5 cm⁻¹
Cond. Band

Fig. 20

Fig. 21

Magnetic field or impurity concentration dependence of the impurity band given by Hasegawa and Nakamura. (After Hasegawa and Nakamura[25].) The impurity band is (a) detached from, (b) just touched to, and (c) merged into the main band.

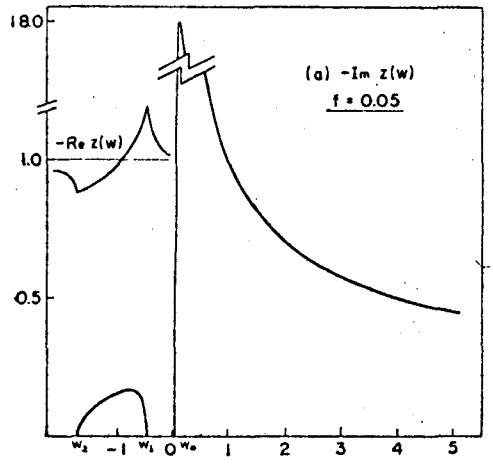
18.0
1.0
0.5
-Re z(w)
(a) -Im z(w)
f = 0.05
w_2 -1 w_1 0 w_0 1 2 3 4 5

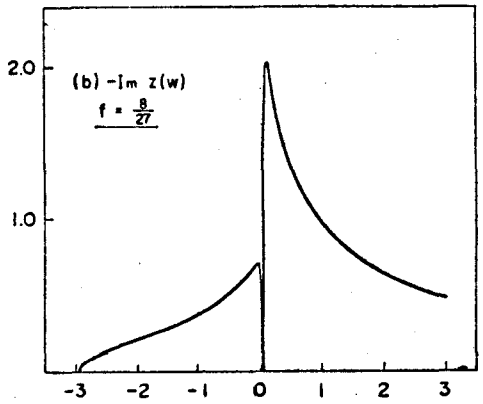
2.0
1.0
(b) -Im z(w)
f = 8/27
-3 -2 -1 0 1 2 3

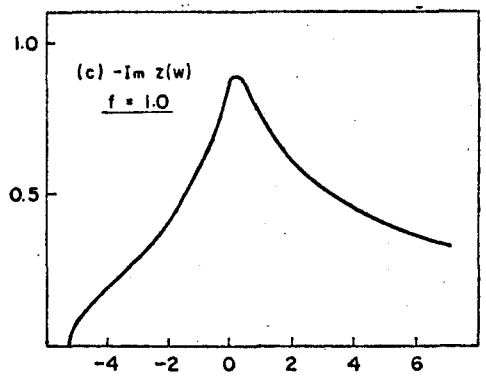
1.0
0.5
(c) -Im z(w)
f = 1.0
-4 -2 0 2 4 6

Fig. 21

Fig. 22

Comparison of the experimental results with the theory of Hasegawa and Nakamura on the phase diagram. For the present result on TE 1715 the separation of impurity band from conduction band was confirmed by the optical spectra and apperance of the activation process was found in transport data. Critical magnetic fields by other investigators are determined from the rising points of Hall coeffecient of electrons as increasing magnetic field. Excess donor concentration, $N_D - N_A$, is used inplace of the real donor concentration, N_D , for the vertical scale to compare with theoretical value.

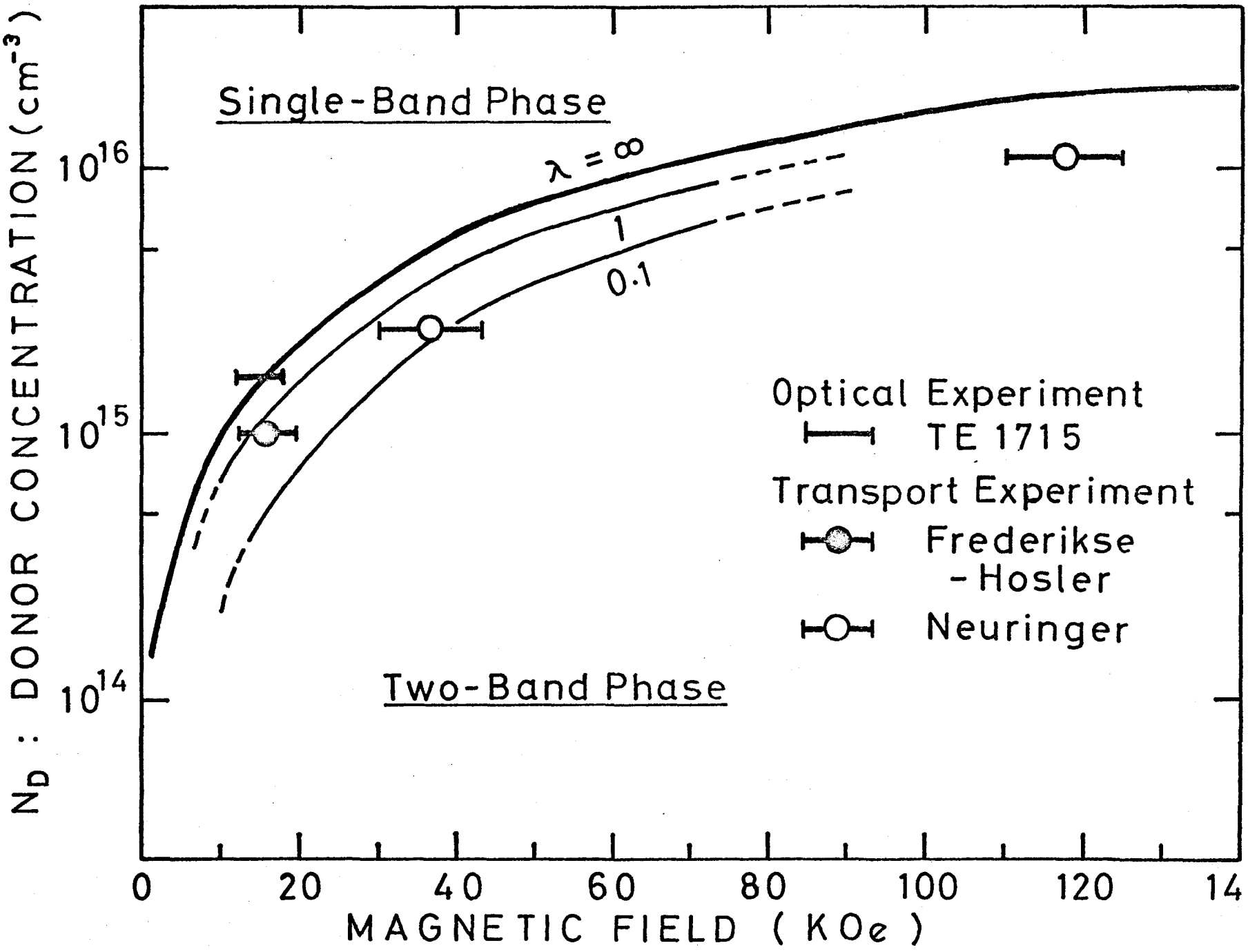
Single-Band Phase
λ = ∞
1
0.1
Two-Band Phase
Optical Experiment
TE 1715
Transport Experiment
Frederikse
-Hosler
Neuringer
N_D : DONOR CONCENTRATION (cm^{-3})
10^{16}
10^{15}
10^{14}
0
20
40
60
80
100
120
140
MAGNETIC FIELD (KOe)

Fig. 22

Paper List

1. Photoconductivity of Antimony-Doped Germanium in the Far-Infrared Region

   K. Nagasaka, Y. Oka, and S. Narita

   Solid State Commun. 5, 333 (1967).

2. Far-Infrared Germenium Detectors

   Y. Oka, K. Nagasaka, and S. Narita

   Japan. J. appl. Phys. 7, 611 (1968).

3. Shallow Impurity States in Germanium under Electrical Breakdown (Short Note)

   Y. Oka and S. Narita

   J. Phys. Soc. Japan 25, 1738 (1968).

4. Far-Infrared Cyclotron Resonance of n-Type InSb under Electric Field

   Y. Oka and S. Narita

   J. Phys. Soc. Japan 28, No.3 (in press)